CENOZOIC CHANGES IN PACIFIC ABSOLUTE PLATE MOTION

A THESIS SUBMITTED TO THE GRADUATE DIVISION OF THE UNIVERSITY OF HAWAI'I IN PARTIAL FULFILLMENT OF THE REQUIREMENTS FOR THE DEGREE OF

MASTER OF SCIENCE

IN

GEOLOGY AND GEOPHYSICS

DECEMBER 2003

By
Nile Akel Kevis Sterling

Thesis Committee:

Paul Wessel, Chairperson
Loren Kroenke
Fred Duennebier

We certify that we have read this thesis and that, in our opinion, it is satisfactory in scope and quality as a thesis for the degree of Master of Science in Geology and Geophysics.

THESIS COMMITTEE

_____

Chairperson

_____

_____

Abstract

Using the polygonal finite rotation method (PFRM) in conjunction with the hotspotting technique, a model of Pacific absolute plate motion (APM) from 65 Ma to the present has been created. This model is based primarily on the Hawaiian-Emperor and Louisville hotspot trails but also incorporates the Cobb, Bowie, Kodiak, Foundation, Caroline, Marquesas and Pitcairn hotspot trails. Using this model, distinct changes in Pacific APM have been identified at 48, 27, 23, 18, 12 and 6 Ma. These changes are reflected as kinks in the linear trends of Pacific hotspot trails. The sense of motion and timing of a number of circum-Pacific tectonic events appear to be correlated with these changes in Pacific APM. With the model and discussion presented here it is suggested that Pacific hotpots are fixed with respect to one another and with respect to the mantle. If they are moving as some paleomagnetic results suggest, they must be moving coherently in response to large-scale mantle flow.

List of Tables

List of Figures

List of Abbreviations

APM	=	Absolute Plate Motion
RPM	=	Relative Plate Motion
HEB	=	Hawaiian-Emperor Bend
PFRM	=	Polygonal Finite Rotation Method
$^{40}Ar/^{39}Ar$	=	Argon Incremental Heating Radiometric Dating Technique
Ma	=	Million Years Ago
km	=	Kilometers
My	=	Million Years
N-MORB	=	Normal Mid-Ocean Ridge Basalt
E-MORB	=	Enriched Mid-Ocean Ridge Basalt
CVA	=	Cumulative Volcano Amplitude
OJP	=	Ontong Java Plateau
EPR	=	East Pacific Rise
TRP	=	Total Reconstruction Pole
DM	=	Differential Motion
S-waves	=	Shear Seismic Waves
P-waves	=	Compressional Seismic Waves
NRM	=	Natural Remenant Magnetization
TRM	=	Thermal Remenant Magnetization
ODP	=	Ocean Drilling Program
APW	=	Apparent Polar Wander
TPW	=	True Polar Wander

Contents

Chapter 1

Introduction

Seamount chains such as the Hawaiian-Emperor are produced as rigid lithospheric plates move over plumes that originate deep in the mantle; Wilson [1963, 1965] coined the term hotspots for these features. The hotspot reference frame has been an attractive reference frame to geologists because it is the most appealing and useful means of measuring absolute plate motions. The validity of this frame of reference hinges on the assumptions of fixed hotspots and rigid lithospheric plates. The fixed hotspot hypothesis [Morgan, 1971, 1972] has explained many observations associated with plate tectonics. Morgan's original hypothesis stated that hotspots were fixed by being rooted in the deep non-convecting mantle. The idea of fixed mantle plumes within a convecting mantle is conceptually hard to grasp, hence many researchers have questioned the validity of the fixed hotspot hypothesis over the past thirty years; this questioning has intensified recently. If mantle plumes do move then we must determine their rates of motion and what the driving forces are; these questions regarding mantle plumes will be central to our understanding of planetary heat

loss and global tectonics. However, if hotspots are fixed with respect to the mantle, they can provide a useful reference frame for plate tectonic analysis. This fixed reference frame can be used to constrain boundary conditions in models of mantle convection and provide a reference frame to which relative plate motions can be tied.

Testing of the fixed hotspot hypothesis has been undertaken using several different approaches. The first approach was to date hotspot trails that appeared to have similar co-polar parallel geometry. Morgan [1971] originally used the geometry of the Hawaiian-Emperor, Tuamotu-Line and Austral-Gilbert-Marshall island chains to convey his idea. He showed that the same motion of the Pacific plate over three fixed hotspots for the past 100 My could generate all three chains. Since then more chains have been discovered and more dates have become available, yet the number of dates is still insufficient to accurately constrain age progressions along these hotspot trails. Another approach to test the fixed hotspot hypothesis has been to use a paleomagnetic frame of reference. The Earth's magnetic field can be approximated by a dipolar magnetic field consisting of a north and south pole. As basaltic rocks crystallize and solidify, magnetite crystals align themselves with the Earth's magnetic field. The orientation of these magnetite crystals can be analyzed to yield a paleomagnetic inclination, which can then be used to solve for the paleolatitude at which the rock crystallized. If hotspots are fixed then all rocks produced at the same hotspot should have the same paleolatitude: the present latitude of the hotspot. Some paleomagnetic studies have concluded that variations in these calculated paleolatitudes indicate true polar wander (TPW) , which simply put is a change in the location of the north and south magnetic poles over time [Besse and Courtillot, 1991; Sager and Koppers, 2000]. Other researchers have

concluded that systematic variations in the paleolatitudes obtained from rocks formed at the same hotspot indicate hotspot drift [Tarduno et al., 2003; Tarduno and Cottrell, 1997; Norton, 1995] . A third approach has been to compare absolute plate motions derived from hotspots on different plates. Using plates linked by seafloor spreading coupled with the constraint of no-net-rotation of the lithosphere, hotspot trends on different plates can be compared. Conclusions based upon this approach have also been mixed depending on whether Pacific and Indo-Atlantic hotspot traces have been considered together by connecting through Antarctica [Molnar and Stock, 1987; Norton, 2000; Cande et al., 1995] or separately [Duncan and Richards, 1991; Muller et al., 1993]. Pacific hotspots appear to be collinear and hotspots on the Indian and Atlantic plates appear to be collinear but the two groups appear to have different trends when compared with each other. Uncertainties associated with all of these approaches leave us with large error bounds on the motion of hotspots, if they do move at all.

As mentioned, Morgan [1971, 1972] was the first to use the geometry and age progressions along the Hawaiian-Emperor, Tuamotu-Line, and the Austral-Gilbert-Marshall chains to develop an absolute plate motion (APM) model for the Pacific plate. He required only two poles of rotation to describe Pacific APM since 100 Ma with a major change in APM occurring at 43 Ma, reflected by the Hawaiian-Emperor bend (HEB). As bathymetric coverage became more complete and the number of isotopic dates from seamounts increased, other Pacific hotspot trails were identified, such as the Cobb-Eickelberger [Turner et al., 1980], Foundation [Mammerickx, 1992], Caroline [Keating et al., 1984], Pitcairn [Duncan et al., 1974] and several other trails. These trails were then incorporated and Pacific

APM models were refined. Many researchers have proposed second-order changes in Pacific APM to account for kinks in Pacific hotspot trails [Duncan and Clague, 1985; Cox and Engebretson, 1985; Pollitz, 1986; Lonsdale, 1988; Kamp, 1991; Wessel and Kroenke, 1997]. Other authors have suggested that kinks in Pacific hotspot trails are the result of hotspot movement, [Norton, 1995; Tarduno and Cottrell, 1997; Cox, 1999; Steinberger, 2000; Koppers et al., 2001; Tarduno et al., 2003]. Thus, the debate over hotspot fixidity rages on.

If hotspots are fixed with respect to the mantle, then changes in APM would produce kinks in the linear trends of the trails. Changes in Pacific APM would also have a major impact on the tectonic regimes around the Pacific rim, including changes in relative plate motions, deformation along plate boundaries, changes in the direction and velocity of subduction and changes in arc volcanism associated with these subduction zones. Clearly, changes in Pacific APM should leave a distinct signature in the geologic record. The timing and sense of motion inferred by these tectonic events can then be correlated with the timing and direction of Pacific APM derived from hotspot trails.

One of the major problems in determining a plate motion model from hotspot produced seamount trails is in determining coeval segments on different trails used for fitting copolar small circles. Due to the scarcity of radiometric dates, picking the end points for each segment based on chronology becomes very difficult. Furthermore, as segments become shorter, the uncertainty in their pole locations becomes very large. To avoid these obstacles, the polygonal finite rotation method (PFRM) [Harada and Hamano, 2000] in conjunction with the hotspotting technique [Wessel and Kroenke, 1997] have been used in this study to

determine an APM model relative to fixed hotspots for the Pacific plate from 65 Ma to the present. The sense of motion and timing of changes seen in the Pacific APM model have also been correlated with tectonic events around the Pacific plate.

Chapter 2

Summary of Hotspot Chains on the Pacific Plate

2.1 Pacfic Hotspots

There are numerous hotspot trails on the Pacific plate (see Figure 2.1). Not all Pacific hotspots have been active as long as the Hawaiian hotspot or have had the same consistent and volouminous delivery of magma to the surface. Many trails have very few dates available, if any. For this reason only the clearest and best dated trails are used in this modeling procedure, including: the Hawaiian-Emperor Seamount Chain, the Louisville Seamount Chain, the Foundation Seamount Chain, the Cobb-Eickelberger Seamount Chain and the Caroline Seamount Chain.

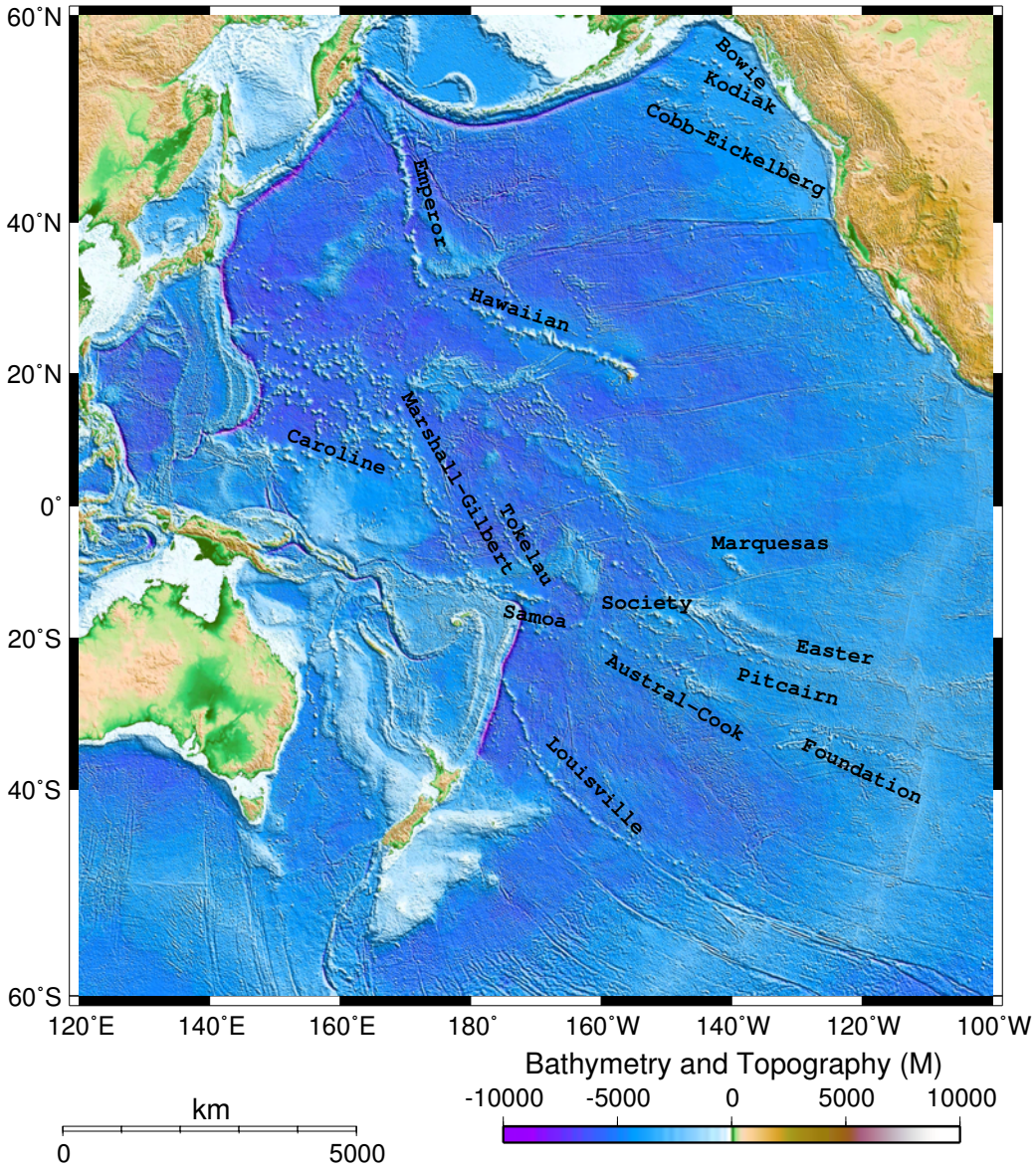

Figure 2.1: Topography of the Pacific region showing names of hotspot-produced seamount chains.

2.2 Hawaiian-Emperor Seamount Chain

The Hawaiian-Emperor seamount chain is the classic example of a hotspot track. It shows clear age progression along its 6100 km trail and contains more than 100 volcanoes. Figure 2.2 shows $^{40}Ar/^{39}Ar$ dates from the Hawaiian-Emperor Seamount Chain. Many theories pertaining to hotspots and plate tectonics have been based upon the Hawaiian-Emperor chain. The chain displays a nearly perfect example of volcanic growth as the plate moves over the hotspot followed by erosion as it moves away from the hotspot. Its intraplate location also makes it an ideal hotspot to study since it is clearly not associated with a spreading ridge nor any other magma source besides the plume itself. Detroit seamount, situated near the Kamchatka-Aleutian cusp is the oldest in the Hawaiian-Emperor chain with an age of 81 Ma [Clague, 1996]. Loihi, an active submarine volcano located 28 km off the southeast coast of the Big Island of Hawaii [Walker, 1990], is the youngest in the chain; presumably it is on the leading edge of the hotspot.

Most Hawaiian volcanoes have four stages of volcanism. Distinct differences in chemistry, the frequency of volcanic events and location of volcanic events with respect to the hotspot are used to characterize the these stages [Moore et al., 1982]. Volcanism begins with the pre-shield stage as virgin oceanic crust moves over the leading edge of the plume. Alkalic lavas including transitional basalt, alkalic basalt and basanite are the main products of this stage and are believed to supply less than 1% of the volume of the volcano. The pre-shield stage is nearly impossible to sample because these lavas are later covered by subsequent stages, therefore these lavas have been the least studied. Loihi may be in

a transitional phase between the pre-shield and shield stages and may be the only place where the pre-shield stage has been sampled [Moore et al., 1982]. The second stage is the shield building stage. Tholeitic basalts are the main product of this stage and may account for nearly 99% of a Hawaiian volcano's volume. Melt production and chemistry suggest that the volcano is located over the central and hottest part of the plume during this stage. This period is characterized by nearly continuous effusive eruptions, occasional explosive eruptions and a large volume of intrusives being emplaced. Kilauea and Mauna Loa are presently in the tholeitic shield-building stage and Loihi may be entering it. The third stage of Hawaiian volcanism is the alkalic-cap or post-caldera stage. When the volcano is located over the trailing edge of the plume, alkalic basalt and associated differentiated lavas erupt to fill the caldera and cap the main shield; this stage accounts for about 1% of the volcanoes volume. Mauna Kea and Hualalai are presently in the alkalic-cap stage. The last stage of volcanism is the post-erosional stage, which may lag behind the shield stage by a few million years and accounts for less than 1% of the volcano's volume. Post-erosional volcanics are generally $Si0_2$-poor, nephelinic-suite lavas that may contain xenoliths. These eruptions are often more explosive than earlier stages and are centered on satellite vents with a frequency of about one every 10 to 20 thousand years. Post-erosional vents are not located over the plume but may be as much as 300 km or more downstream from the plume. This volcanism along the Hawaiian-Emperor chain may be related to the volcano riding over the Hawaiian Arch, a flexural arch produced by down-warping of elastic lithosphere by the load of the youngest and largest volcano in the chain [ten Brink and Brocher, 1987]. Ribe and Christensen [1999] proposed that post-erosional volcanism might be associated with

a second melting anomaly produced by plume flow interacting with a moving lithosphere. They suggest that this melting anomaly is centered 400 km behind the plume. The physical mechanism for melting could be flexure, flow related or most likely a combination of both. The Honolulu volcanic series is an example of the post-erosional stage of volcanism. This model of the evolution of a Hawaiian volcano has been well documented; of course there are occasional variations and not all Hawaiian volcanoes evolve identically. The growth of a Hawaiian volcano is thought to last approximately 1 million years [Moore and Clague, 1992]. The different stages become important when trying to assign a certain volcano with an age. In practice, it is hard to sample the early stages of volcanism; therefore most dates probably come from volcanism that occurred late in the volcanoes' growth. Ideally, a date for the tholeitic shield building stage would be the most useful for APM modeling because it should represent the time that the volcano was located directly over the hotspot. Dates from other stages of volcanism, especially the post-erosional stage do not represent the period the volcano was directly over the hotspot and can throw off the chronology of an APM model. These changes in chemistry and many other characteristics of Hawaiian volcanoes have been identified on other hotspot-produced volcanoes as well [Keating et al., 1984].

Hawaiian volcanoes and the Hawaiian plume have been more thoroughly studied than any other seamount chain, yet the present location of the plume is still debated by many scientists. Physical volcanology suggests that the central portion of the plume is located closest to Mauna Loa Volcano. In historical times Mauna Loa has erupted a far larger volume of lava than Kilauea and Loihi, even after the ongoing $\sim$20 year eruption at Kilauea has been accounted for [Trusdell, 2002]. Seismicity suggests that the central portion of the

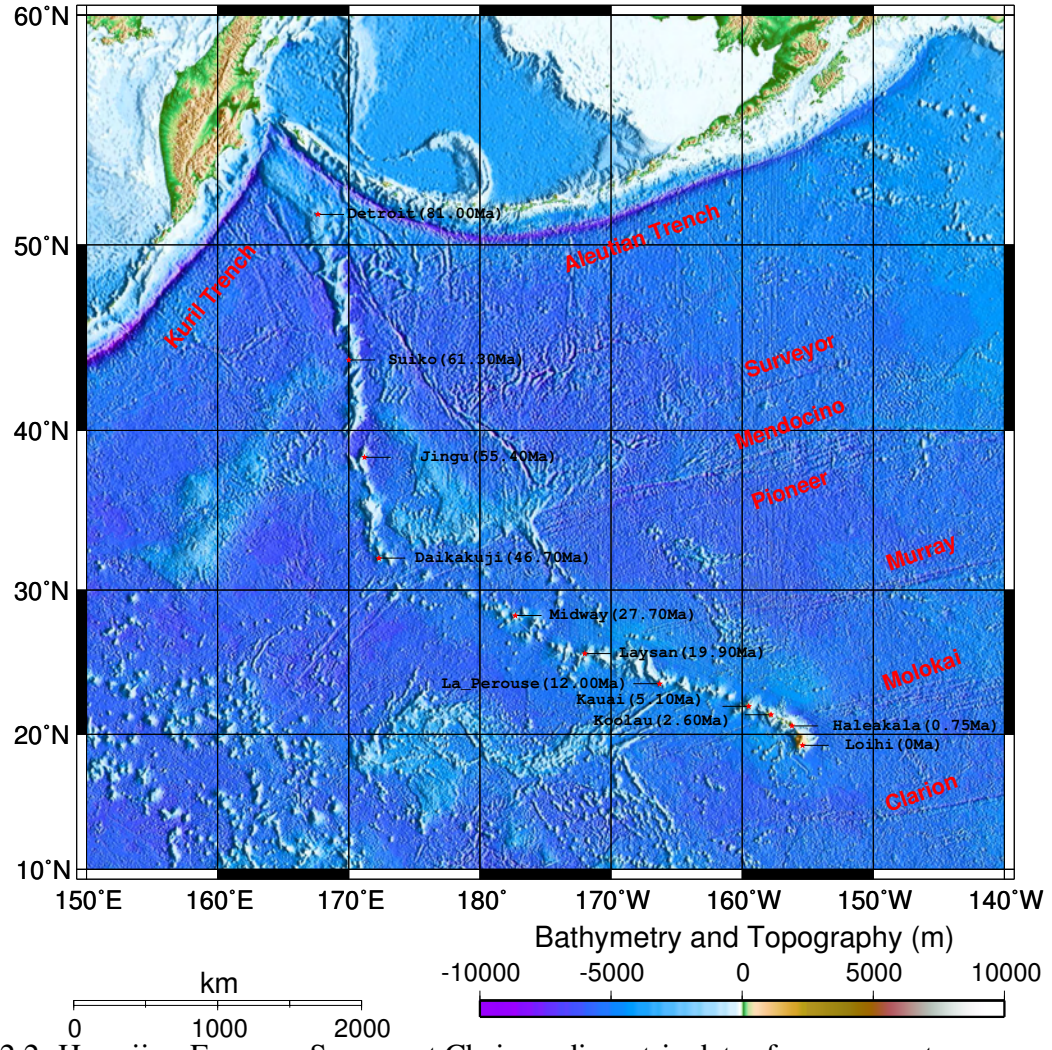

Figure 2.2: Hawaiian-Emperor Seamount Chain; radiometric dates for seamounts shown in black. Names of fracture zones are labelled in red. Also shown are the Aleutian and Kuril trenches.

plume may be located closer to Kilauea because earthquakes at depth may define a central conduit deep beneath Kilauea [Ryan, 1988]. Different types of geochemical studies also have varying results on where the center of the plume is located. Major element chemistry suggests it is closest to Mauna Loa [Rhodes, 2002], whereas Helium isotope chemistry suggests it may be closer to Loihi [Kurz, 2002].

2.3 Louisville Seamount Chain

The Louisville seamount chain is a 4300 km long hotspot trail extending from the Tonga-Kermadec trench towards the Pacific-Antarctic Ridge. The chain is made up of more than 60 volcanoes spaced approximately 100 km apart. Figure 2.3 shows $^{40}Ar/^{39}Ar$ ages of seamounts in the chain which range from 68.35 Ma at the northwest end of the chain to 0.5 Ma at an isolated unnamed seamount at the southeast end of the chain [Lonsdale, 1988]. Production of melt from the Louisville hotspot appears to have decreased substantially since around 20 Ma. Seamounts produced by the hotspot since 20 Ma have been smaller and spaced farther apart then seamounts formed prior to 20 Ma. The present location of the hotspot is unclear because there is no active volcano at the southeast end of the chain. The Louisville hotspot may no longer be active, or the hotspot could be under the nearby Pacific-Antarctic Ridge. Lonsdale [1988] suggests the hotspot is located close to a small

undated seamount located at (138.1^0 W, 50.9^0 S). Wessel and Kroenke [1997] suggest that the hotspot may be located further south near Hollister Ridge, while others have proposed an intermediate location in the Eltanin fracture zone system [Koppers et al., 2001].

2.4 Foundation Seamount Chain

The Foundation Seamounts form a 1400 km long trail of volcanism on the Pacific plate. The oldest seamount in the chain dated at 21.20 Ma is located at approximately (131^0 W, 33^0 S). The chain extends southeastward to the Pacific-Antarctic Ridge, ending at approximately 38^0 S (see Figure 2.4). The hotspot appears to have been active in the very recent geologic past but there is presently no active volcano at the southeast end of the chain. Activity of the Foundation plume has waned in the last few million years; the plume may actually be in the process of dying out. Several researchers, [Mammerickx, 1992; Devey et al., 1997; Hekinian et al., 1997; O'Connor et al., 1998, 2001] have concluded that the Foundation hotspot has been complexly interacting with the Pacific-Antarctic Ridge for most of its existence. The Pacific-Antarctic spreading ridge has been systematically migrating towards the Foundation hotspot for at least the past 21 My. This ridge migration was temporarily interrupted by the formation of the Selkirk microplate that is located in the western portion of the chain [O'Connor et al., 1998; Devey et al., 1997; Hekinian et al., 1997]. The Foundation plume has been strongly influenced by the Pacific-Antarctic spreading ridge during the past 6 My, forming ridges perpendicular to the spreading axis that most likely are the result of magma from the plume being channeled to the ridge [O'Connor et al., 1998, 2001; Devey

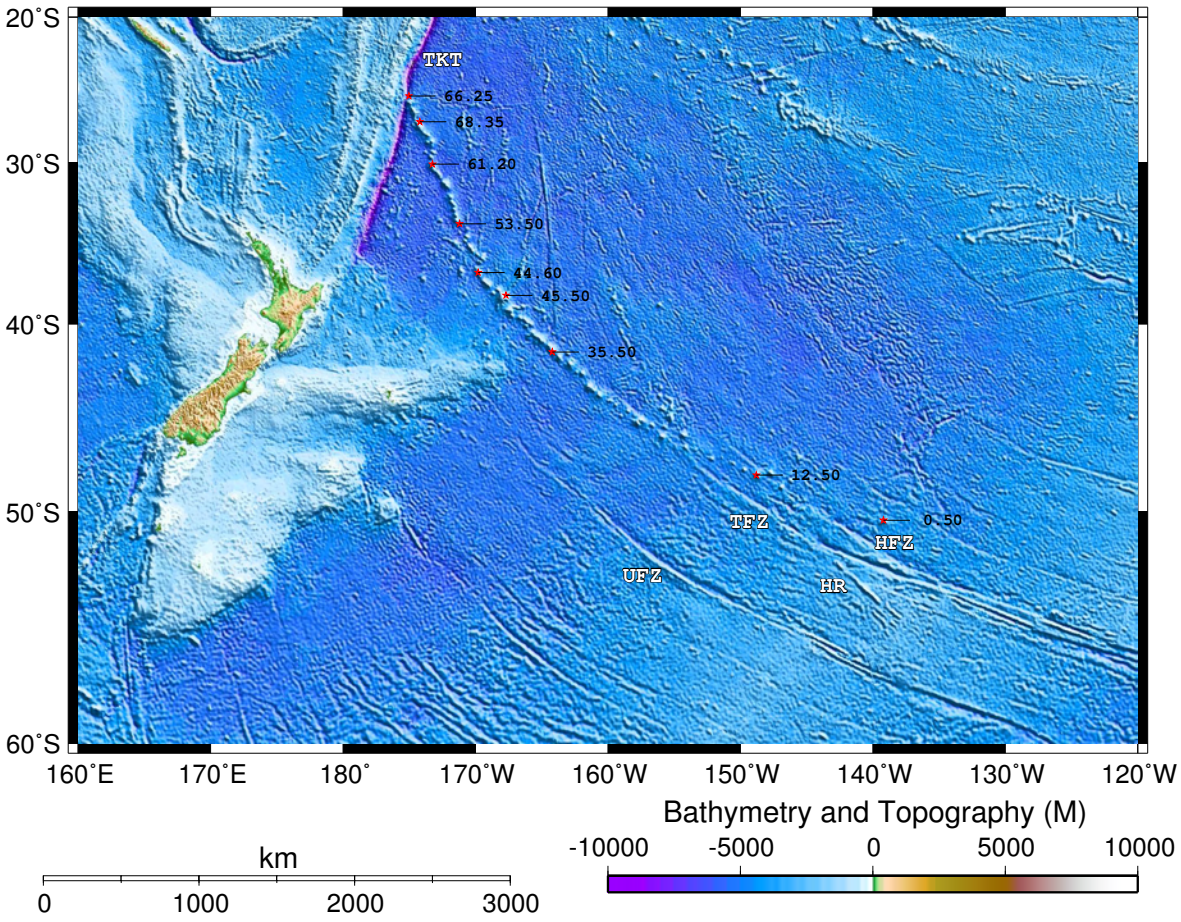

Figure 2.3: Louisville Seamount Chain; radiometric dates for seamounts shown in black. Also labeled is the Tonga-Kermadec Trench (TT), Hollister Ridge (HR), Udintsev Fracture Zone (UFZ), Tharp Fracture Zone (TFZ) and the Heezen Fracture Zone (HFZ).

et al., 1997]. The chemistry of lavas dredged from the chain also suggests varying amounts of interaction through time between the two magma sources [Hekinian et al., 1997].

2.5 Cobb-Eickelberg Seamount Chain

The Cobb-Eickelberg Seamount Chain shown in Figure 2.5 is located in the northeast Pacific. The chain is approximately 2000 km long and contains 40 seamounts. The chain has linear age progression, the oldest seamount in the chain is Patton seamount dated at 29.26 Ma. The youngest seamount in the chain is Axial volcano, located at the intersection of the Juan De Fuca Ridge and the Cobb-Eickelberg hotspot trail. Axial volcano rises well above the surrounding ridge up to 1500 meters below sea level; the ridge is approximately 2200 meters below sea level. Axial volcano is presently active with the last known eruption occurring on January 25th, 1998 [Baker et al., 1999]. The Cobb hotspot has been interacting with the Juan de Fuca Ridge for at least the past 7 My [Karsten and Delaney, 1989]. The hotspot may be directly beneath the ridge axis now or slightly off axis with all of its output being channeled to the ridge. Axial volcano has erupted two distinct types of lavas both being transitional between normal mid-ocean ridge basalt (N-MORB) and enriched mid-ocean ridge basalt (E-MORB). There is no evidence for substantial volumes of mantle plume like magmas associated with the Cobb hotspot. The lavas erupted from Axial volcano are similar to those erupted along the rest of the Juan De Fuca Ridge. There are subtle differences in axial lavas compared to those of adjoining ridge segments. Rhodes et al. [1990] suggests these are due to differences in melting, not differences in sources. This

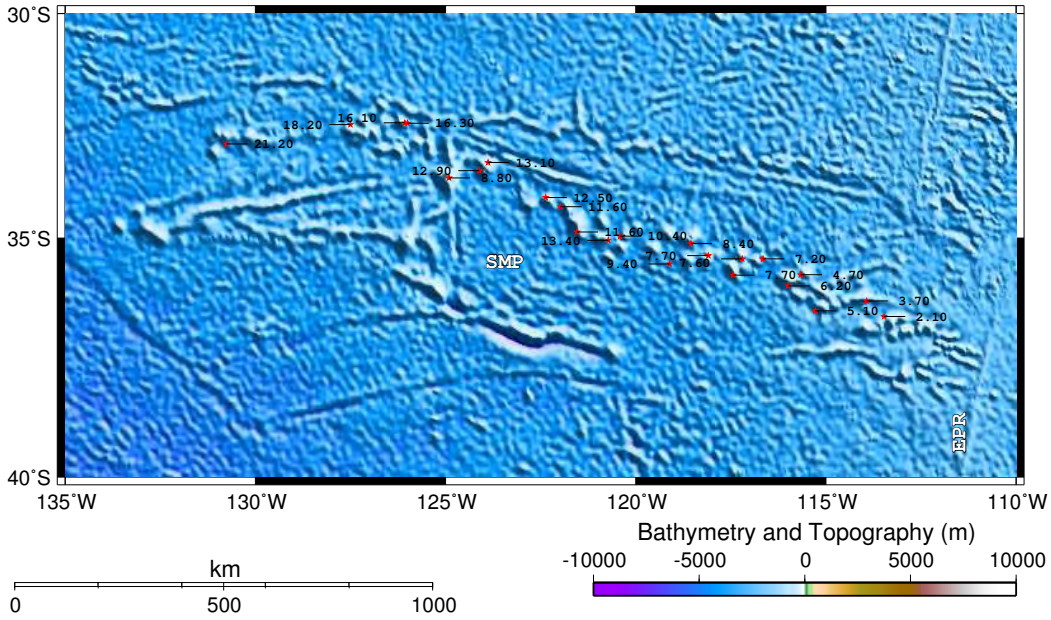

Figure 2.4: Foundation Seamount Chain; radiometric dates for seamounts shown in black. The East Pacific Rise (EPR) and the Selkirk microplate (SMP) are also labeled.

chemistry suggests that the Cobb Hotspot may represent a thermal anomaly rather than a thermal and chemical anomaly like the Hawaiian hotspot. This may be due to differences in the region of the mantle from which the two hotspots originate. Axial volcano represents a large mass excess when compared to the rest of the ridge and this is associated with a melting or thermal anomaly [Johnson and Helferty, 1990]. Even with no distinct chemical signature, it seems that Axial volcano is being influenced by the Cobb hotspot and the hotspot is most likely under Axial volcano.

2.6 Caroline Seamount Chain

The Caroline Seamount Chain, shown in Figure 2.6, is located in the western Pacific Ocean and trends roughly east to west from the Mariana trench to the Melanesian Basin. It is comprised of approximately 10 hotspot-produced seamounts and islands that span 1500 km. Ages for the Caroline trail show a linear progression and range from 10.6 Ma at Truk in the west to 1.8 Ma age for Kusaie in the east. The petrography and geochemical evolution of lavas are similar to that of Hawaiian volcanoes [Mattey, 1982]. The dominant shield-building lavas in the Caroline Seamount chain are part of a differentiated alkalic series rather than tholeitic lavas. Petrographic and geochemical cahracteristics of Caroline shield lavas reveal a general shift towards more alkaline lavas with time [Mattey, 1982]. Keating et al. [1984] observed that the size of the islands has diminshed with time and concluded that the Caroline hotspot was waning in strength over last 11 my. There is no

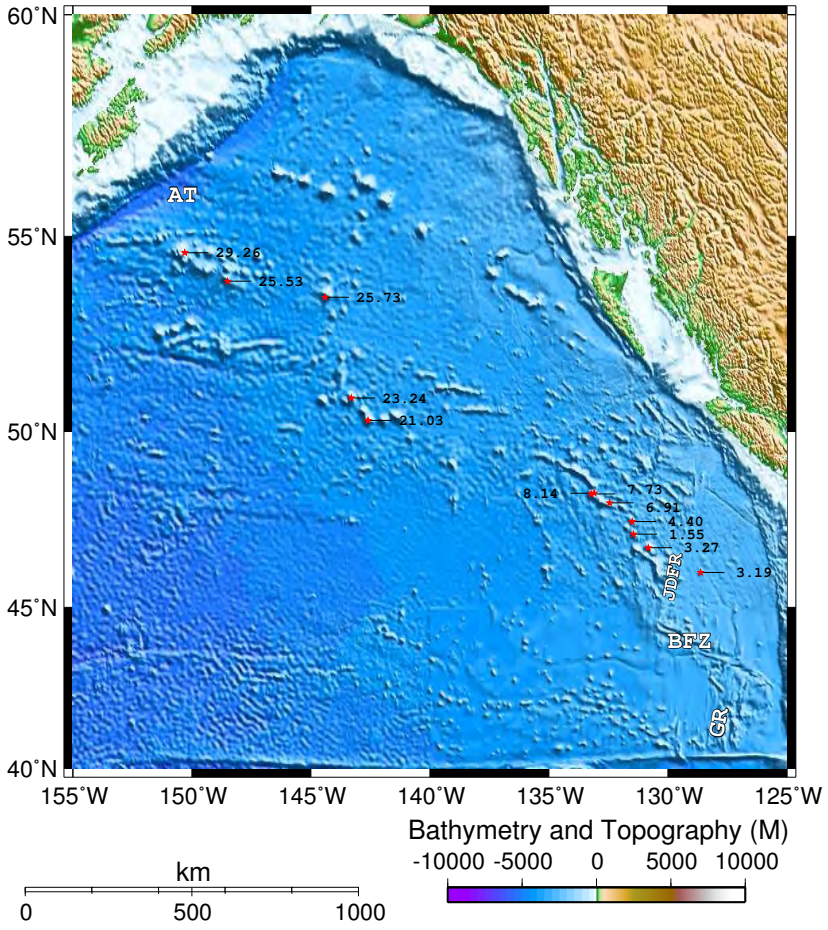

Figure 2.5: Cobb-Eickelberg Seamount Chain; radiometric dates for seamounts shown in black. Also labeled are the Aleutian Trench (AT), Juan de Fuca Ridge (JDFR), Blanco Fracture Zone (BFZ) and the Gorda Ridge

active volcano in the chain, so the present hotspot location is unknown. The Caroline hotspot may be extinct.

2.7 Other Pacific Hotspot-Produced Seamount Chains

There are many more Cenozoic hotspot-produced seamount chains on the Pacific Plate than those mentioned above. The available dates and geometry from many of these chains appear to match the trends of those previously discussed (see Figure 2.1). The Marquesas chain, located in the central Pacific, has linear age progression along approximately 10 seamounts and islands ranging in age from ∼6-0 Ma. Just south of the Marquesas trail is the Pitcairn hotspot trail. It ranges in age from 12-0 Ma, with active volcanism at the southeastern end. The Tokelau trail is located in the west central Pacific. There are no dates from the Tokelau trail but the geometry matches the Emperor stage of the Hawaiian-Emperor chain. The Marshall-Gilbert Chain is just west of the Tokelaus, it also matches the geometry of the Emperor stage. The Samoa trail has ages from 27-0 Ma but other magma sources may have contributed in its formation. The Society Islands are hotspot produced and range in age from ∼4.5-0 Ma. The Austral-Cook seamount trail in the south central Pacific ranges in age from 12-1.5 Ma.

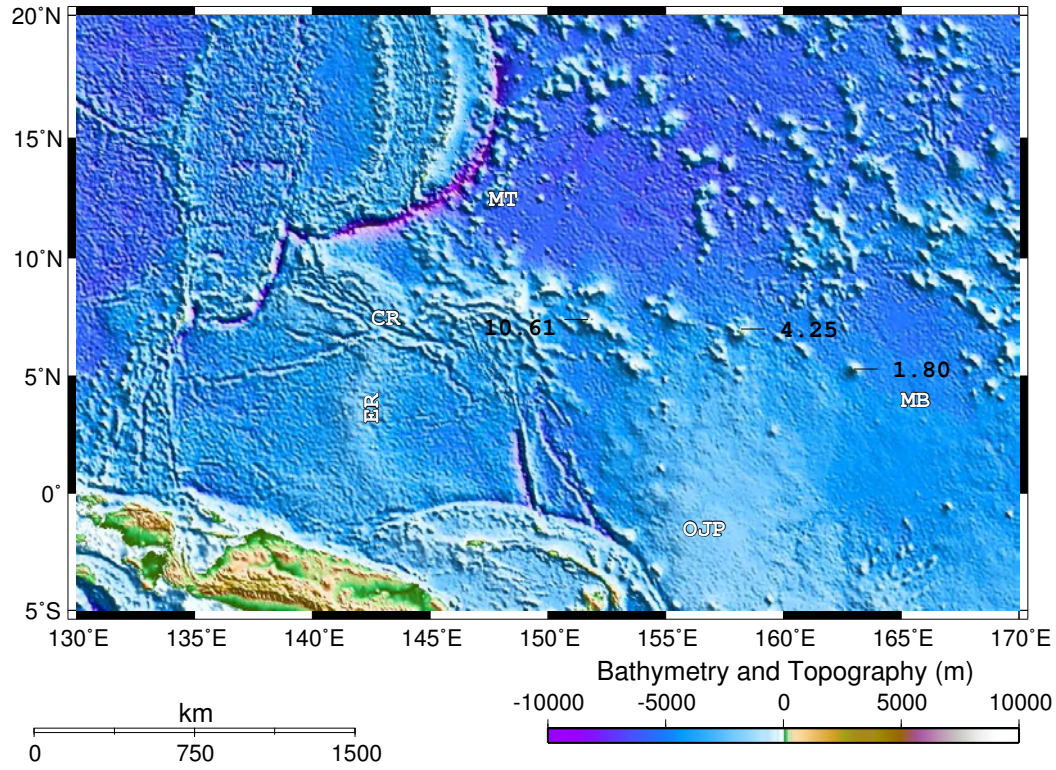

Figure 2.6: Caroline seamount chain; radiometric dates for seamounts shown in black. Also labeled are the Mariana Trench (MT), the Caroline Ridge (CR), the Euripik Ridge (ER), the Ontong Java Plateau (OJP) and the Melanesian Basin (MB).

Chapter 3

Paleomagnetics

3.1 Background

The Earth's magnetic field is generally thought to be created by dynamo action in the fluid outer core. The outer core extends from a depth of 2881 to 5150 km; it is bounded above by the solid lower mantle and below by the solid inner core. The outer core has been defined in terms of its seismic properties and has never been physically sampled. We know the outer core is in a liquid state because of the way seismic waves created by earthquakes interact with it. Shear waves (S-waves) do not penetrate the outer core because it is liquid and liquids cannot be sheared. Its composition has been deduced from matching its known seismic velocities derived from compressional P-waves with the velocities of alloys produced in the laboratory and tested under core pressures. The outer core is thought to be primarily composed of an iron-nickel alloy with a small percentage of lighter elements including sulfur, oxygen, and hydrogen. The field created by this dynamo action can be well

modeled as an axial dipole. The axis of this dipole closely matches the Earth's spin axis, intersecting the Earths surface at roughly the north and south poles. About 90% of the magnetic field measured at the Earth's surface can be described by an axial dipole tilted 11.5^0 with respect to the rotation axis. The remaining 10% of the magnetic field is nondipolar at the surface. The Earth's magnetic field is clearly dynamic: historic magnetic data suggests that the orientation of the dipole component of the field has drifted westward at about 0.05^0 per year and the nondipole portion of the field has been drifting at a rate of approximately 0.18^0 per year. The strength of the field also varies with time, over the past 3000 years it has decreased by one third. Changes in the magnetic field with periods from 1 yr to 10^5 yr are termed geomagnetic secular variation. The polarity of the dipole portion of the magnetic field also reverses approximately every 350,000 years [Tivey, 2002]. Presently, magnetic flow lines come out of the south pole and go into the north pole, the field in this state has been termed a normal period. When the flowlines go in the opposite direction it is termed a reversed period. In paleomagnetism, the Earth's magnetic field is defined by the orientation of vectors that represent the strength and direction of the field at any spot on the surface of the Earth. The total magnetic field vector ($\mathbf{H}$) can be broken into two components, a vertical component $\mathbf{H}_v = \mathbf{H}\sin(\mathrm{I})$ and a horizontal component $\mathbf{H}_h = \mathbf{H}\cos(\mathrm{I})$. Inclination, I, is the vertical angle, i.e. the dip between the horizontal and $\mathbf{H}$. Declination, D, is the azimuthal angle between the horizontal component of $\mathbf{H}$, i.e., $\mathbf{H}_h$ and geographic north. The component of the magnetic field in the geographic north direction is $\mathbf{H}\cos(\mathrm{I})\cos(\mathrm{D})$; the east component is $\mathbf{H}\cos(\mathrm{I})\sin(\mathrm{D})$ [McElhinney, 1973].

If magnetic minerals are free to move around they will orient themselves with the Earths magnetic field, essentially acting similar to the needle on a compass. The only difference being that the compass needle is fixed in the horizontal plane and is not affected by the vertical component of the magnetic field, whereas the mineral would be free to align itself with the vertical portion of the field as well as the horizontal. In practice the only magnetic minerals that are free to move in this fashion are sediments as they are being deposited prior to being fixed due to compaction and volcanic magma prior to solidifying. Natural remenant magnetism (NRM) is remenant magnetization present in a rock sample and depends on the geomagnetic field and geologic processes during rock formation, which is termed primary NRM and during the history of the rock, which is termed secondary NRM. It is natural remenant magnetization that is of concern in paleomagnetics. There are three general types of NRM: 1) thermoremenant magnetization, acquired during cooling from high temperatures; 2) chemical remenant magnetization, formed by growth of ferromagnetic grains below the Curie temperature; and 3) detrital remenant magnetization, acquired during accumulation of sedimentary rocks containing detrital ferromagnetic minerals. Here we are mainly concerned with igneous rocks and more specifically basalts, which clearly fall under the category of themoremenant magnetism (TRM). As basaltic magma cools in the presence of the Earth's magnetic field magnetite grains align themselves with the field and produce a remanant magnetization. At regular Earth surface temperatures this remnant magnetization can be stable over geologic time periods and resistant to effects of weak magnetic fields after original cooling. This is an extremely simplified explanation of the

Earth's magnetic field and how this field influences magnetic minerals but it should suffice for this discussion.

Now consider a stationary hotspot fixed with respect to the mantle. As basaltic magma cools the magnetite grains within the basaltic rocks align themselves with the Earth's magnetic field. If these rocks have not been altered by any magnetic fields after solidifying and have not undergone any deformation they can yield valuable information regarding the location of the hotspot at the time the rocks solidified. By carefully sampling and analyzing these rocks it is possible to attain the magnetic inclination and declination they acquired while solidifying. The declination is of no real use in plate tectonics because it is non-unique, meaning that we cannot derive a longitude of formation from it. On the other hand, the inclination obtained through this analysis can be used to derive the paleolatitude at which the rocks solidified. If a hotspot is fixed with respect to the mantle all rocks formed at the hotspot should have roughly the same inclination and therefore the same paleolatitude. By sampling and determining paleolatitudes from samples collected along the length of a hotspot trail it is possible to test hotspot fixidity using paleomagnetic data.

3.2 Polar Wander

True Polar Wander (TPW) is defined as the rotation of Earth's spin axis with respect to the mantle. It has been suggested that TPW may be the result of changes in the Earth's maximum principal axis of inertia caused by redistribition of mass in the mantle [Goldreich and Toomre, 1969]. Apparent Polar Wander (APW) is defined as motion of the Earth's spin

axis with respect to a fixed plate. A sequence of paleomagnetic poles from a single plate for certain time period is defined as an APW path. APW paths can be easily inverted to represent plate motion relative to a fixed rotation axis. By definition APW = APM + TPW. If a hotspot is stationary, no TPW has occured and the Earth's dipole is centered on 90^0 N. The volcanic track produced by the hotspot will perfectly match the APW path for the plate. Also, if we rotate the paleomagnetic poles back using rotation parameters derived from a hotspot reconstruction all paleomagnetic poles will rotate back to the pole at 90^0 N [Torsvik et al., 2002]. These are standard tests used to analyze the fixity of hotspots and the dipole. If a hotspot or the location of the dipole moves over the time being considered there will be a mismatch with these tests.

3.3 A Paleomagnetic Test of Hotspot Fixidity

Such an analysis has been done using paleomagnetic data gathered along the Hawaiian-Emperor hotspot trail. The purpose of ODP Leg 197 was to conduct a systematic paleomagnetic testing of the fixity of the Hawaiian hotspot [Tarduno et al., 2003]. In August 2001 the JOIDES Resolution drilled three holes along the Emperor portion of the Hawaiian-Emperor hotspot trail. Figure 3.1 shows paleolatitudes gathered along the chain. Hole 1204B was drilled on the northern end of the summit platform of Detroit seamount located at (51^0 11.64' N 167^0 46.42' E). Tholeitic basalt basement was penetrated and recovered. Paleomagnetic inclinations obtained from the core have a mean inclination of 58.9^0 $+5.8^0$/-6.4^0. The Paleolatitude derived from these inclinations is 39.7^0 N $+4.4^0$/-3.7^0. However,

the angular dispersion of the data obtained indicates that the full range of geomagnetic secular variation important for obtaining high-resolution paleolatitudes was not sampled. ODP hole 1205 was drilled on the northwestern edge of Nintoku seamount at 41.3^0 N. The rock cores recovered from this hole were of a similar chemistry to that of post-shield volcanics from Mauna Kea volcano on the Big Island of Hawaii. Twenty-two separate independent inclination groups were obtained from the core. The mean inclination is -45.7^0 +10.5^0/-6.3^0 and the paleolatitude derived from this is 27.1^0 N +5.5^0/-7.7^0. ODP hole 1206 was drilled on the southeast side of the lower terrace of Koko seamount at (34^0 55.55' N, 172^0 8.75' E). Rocks recovered from the core were tholeitic basalts. Fourteen independent inclination groups were recovered with a mean inclination of 38.50^0 +8.40^0/-10.90^0 which corresponds to a mean paleolatitude of 21.70^0 N +6.40^0/-7.00^0. The paleolatitudes derived for Detroit, Nintoku, and Koko seamounts are $\sim$20^0, 8^0 and 2^0 respectively north of the present location of the Hawaiian hotspot. The results from ODP leg 197 suggest that the Hawaiian hotspot migrated approximately 20^0 degrees to the south between 81 and 48 Ma and became fixed with respect to the mantle at its present location of $\sim$155.4^0 W, 19^0 N at 48 Ma located.

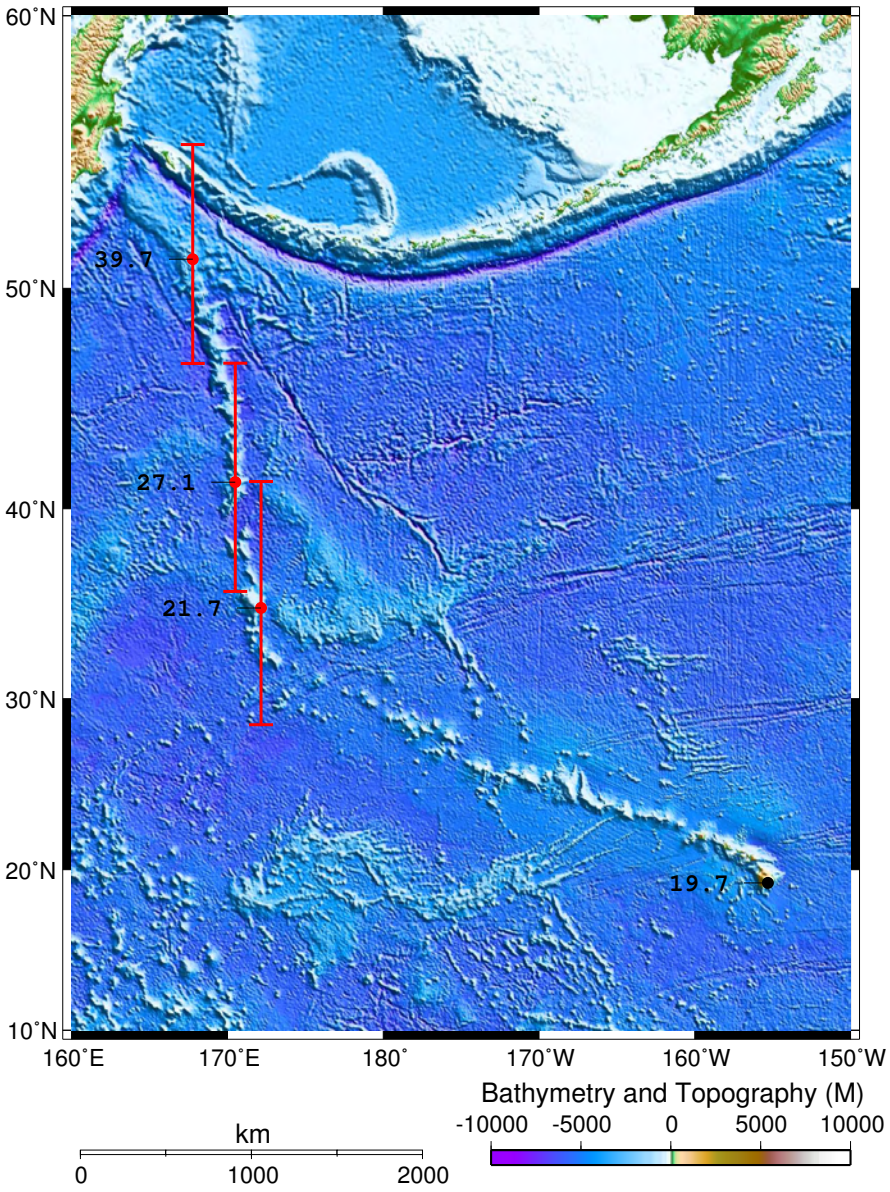

Figure 3.1: Hawaiian-Emperor seamount chain; paleolatitiudes from ODP leg 197 shown in red with error bars and present latitude of the Hawaiian hotspot shown in black.

Chapter 4

Modeling of Absolute Plate Motions

4.1 Background

The kinematic theory of plate tectonics is based upon Euler's theorem that motions on a sphere can be expressed as a rigid rotation about an axis. With the use of Euler's theorem and spherical trigonometry we can mathematically describe the movements of lithospheric plates on the surface of the Earth. Applying the PFRM and hotspotting to a Pacific seamount database [Wessel and Lyons, 1997] created from satellite-derived bathymetry [Sandwell and Smith, 1997] a model of Pacific APM has been created as described in the following sections.

4.2 Rotation of Plates on a Sphere

The motion of a lithospheric plate (A) on the surface of a spherical approximation of Earth can be described by a rotation, Ω which defines the amount of rotation about an axis that goes through the center of the Earth and intersects the surface at a specific longitude and latitude (ϕ, λ); this point of intersection is defined as the Euler pole ($\mathbf{E}$). Thus, the motion of any point on the plate rotated about the Euler pole ($\mathbf{E}$) with an opening angle of Ω moves along a small circle centered on ($\mathbf{E}$). When the rotation is complete a point $\mathbf{X}$ 90^0 from ($\mathbf{E}$) will have moved along a great circle an angular distance Ω where a positive value of Ω indicates counterclockwise rotation (see Equation 4.1). This motion is known as a finite rotation. Figure 4.1 illustrates point $\mathbf{X}$ on plate A rotated 80 degrees about an Euler pole located at (170 W, 60 N). Symbolically, we write

$$\text{ROT} = (\mathbf{E}, \Omega) \tag{4.1}$$

A series of finite rotations can be used to describe the movement of a plate over time. It is important to note that finite rotations are not vectors, and more importantly they are not commutative; this becomes important in the modeling procedure described below (see Equation 4.2). The rotation obtained by a series of finite rotations depends upon the sequence in which the rotations are applied. Thus, in general,

$$\text{ROT}_A + \text{ROT}_B \neq \text{ROT}_B + \text{ROT}_A \tag{4.2}$$

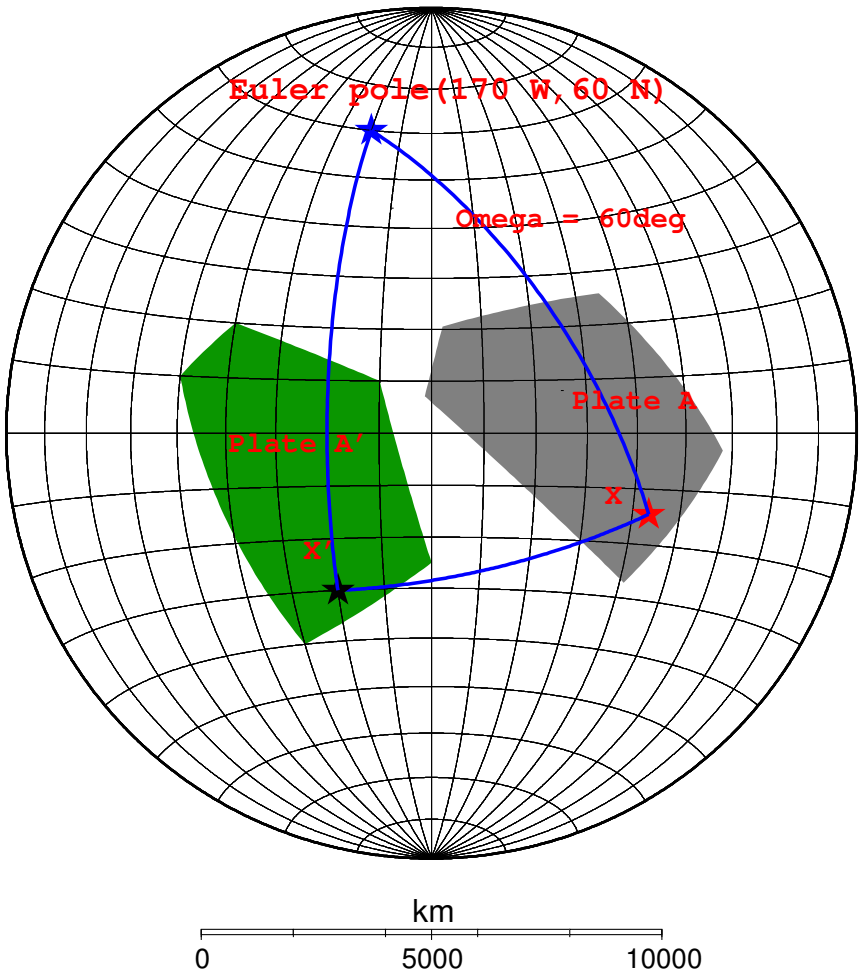

Figure 4.1: Plate A has been rotated 80 degrees about an Euler pole located at (170 W, 60 N) ending up in the position of Plate A'. The point **X** which is 90 degrees from the pole has moved along a great circle an angular distance of 80 degrees

Finite rotations themselves are purely geometric and have no temporal value associated with them. These rotations, when associated with a period of time are termed stage poles, a stage is simply some interval of time in the history of the plate and a stage pole simply defines the sense of motion and the amount of rotation that occurred during the stage. In general practice, it is assumed that the Euler pole remains fixed during a stage and then jumps between successive stages. If a lithospheric plate moves as described above over a hotspot that is fixed relative to the mantle, the hotspot will create a line of volcanism that follows the trace of a small circle about an Euler pole. This trace of volcanism can then be used to determine the Euler pole and opening angle that describes the plates motion relative to the fixed hotspot i.e., absolute plate motion.

4.3 Stage Poles Versus Total Reconstruction Poles

In tectonic analysis several types of poles and rotations are used and it is very easy to become confused about nomenclature. Total reconstruction poles (TRP) are commonly used in relative plate motion (RPM) models and are also used with the PFRM. Stage poles are generally used in traditional APM models. A total reconstruction rotation is defined as a rotation that rotates a point from its present location to its position when it was formed. As an example lets consider the Hawaiian-Emperor Seamount Chain and Morgan's original APM model.

In Figure 4.2 Daikakuji seamount (S1) is located near the Hawaiian-Emperor Bend (HEB). The rotation pole that rotates Daikakuji back to the hotspot is defined as a TRP

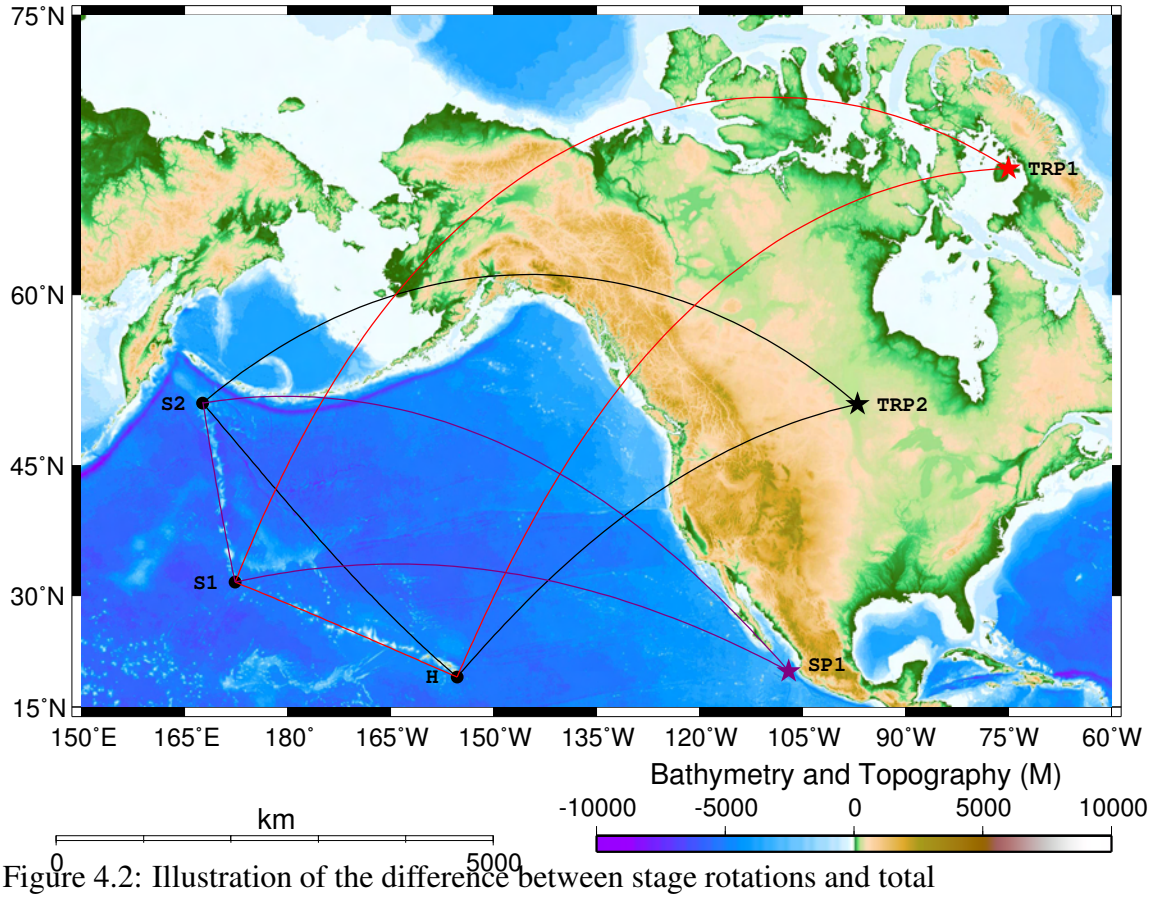

Figure 4.2: Illustration of the difference between stage rotations and total reconstruction rotations. The red star is the total reconstruction pole (TRP1) for Daikakuji seamount (S1) and the red lines are its total reconstruction rotation. The black star is the total reconstruction pole (TRP2) for Detroit seamount (S2) and the black lines are the its total reconstruction rotation. The purple star is the stage pole (SP1) for the Emperor segment of the Hawaiian-Emperor seamount chain (S2) and the purple lines are the Emperor stage rotation. (H) is the Hawaiian hotspot.

because it rotates the seamount back to its position when it was formed; the red star is the pole location (TRP1) and the red lines are the associated rotation. Similarly, the rotation pole that rotates Detroit seamount (S2) back to the hotspot (H) is a total reconstruction pole; the black star is the pole location (TRP2) and black lines represent the rotation in Figure 4.2. If we were to take the mathematical difference between these two TRPs, the result would be the stage pole for the Emperor segment of the seamount chain, the purple triangle (SP1) is the stage pole and purple lines are the associated rotation in Figure 4.2. In this example the Daikakuji total recontruction pole (TRP1) would also be the stage pole for the Hawaiian segment because it not only rotates Daikakuji back to its origin but it is also the first stage in Morgan's model which only used two stages. It is very easy to derive stage poles from total reconstruction poles and vice versa using simple spherical trigonometry operations. As mentioned, total reconstruction poles are genrerally used for RPM modeling. In relative plate motion analysis total reconstruction poles are chosen so that points lying along isochron boundaries all rotate back to their origin, i.e., the ridge axis.

4.4 Least Squares Technique

A least squares technique is generally used to determine the best Euler pole for coeval segments of hotspot chains which define stages in an APM model. The pole location will be chosen such that the misfit, measured as the sum of the squared distance between each seamount and the local small circle, is minimized (see Figure 4.3). One significant draw-

back to this least squares technique is the difficulty in identifying the same stage on separate seamount trails which in turn defines the seamounts to be used in the least squares calculation. The Hawaiian-Emperor bend is an excellent example of this, as the change in the trend of the trail is obvious and fairly well dated. Therefore, defining two separate segments is easy. If less dates are available and the change in trend is not so pronounced, such as along the Louisville chain in the South Pacific, identifying separate segments becomes much more difficult. In the absence of dates, choosing segments may simply not be possible. When using several poorly dated hotspot trails the problem of choosing coeval segments on each trail is compounded, leading to large uncertainties in the rotation parameters (see Figure 4.4).

4.5 Polygonal Finite Rotation Method

Recently, Harada and Hamano [2000] developed a new geometric technique to determine absolute plate motions from hotspot trails. The Polygonal Finite Rotation Method is superior to the standard least squares technique because it is not based on choosing coeval segments of hotspots trails. If hotspots are fixed with respect to the mantle and each other then the distance between hotspots remains the same over time. For instance, consider the locations of seamounts that were formed at three different hotspots at 30 Ma. If these three hotspots have remained fixed with respect to each other from 30 Ma to the present these seamounts will now sit at the vertices of a polygon that is identical to the one defined by the present locations of the hotspots; the only difference being the former polygon has been ro-

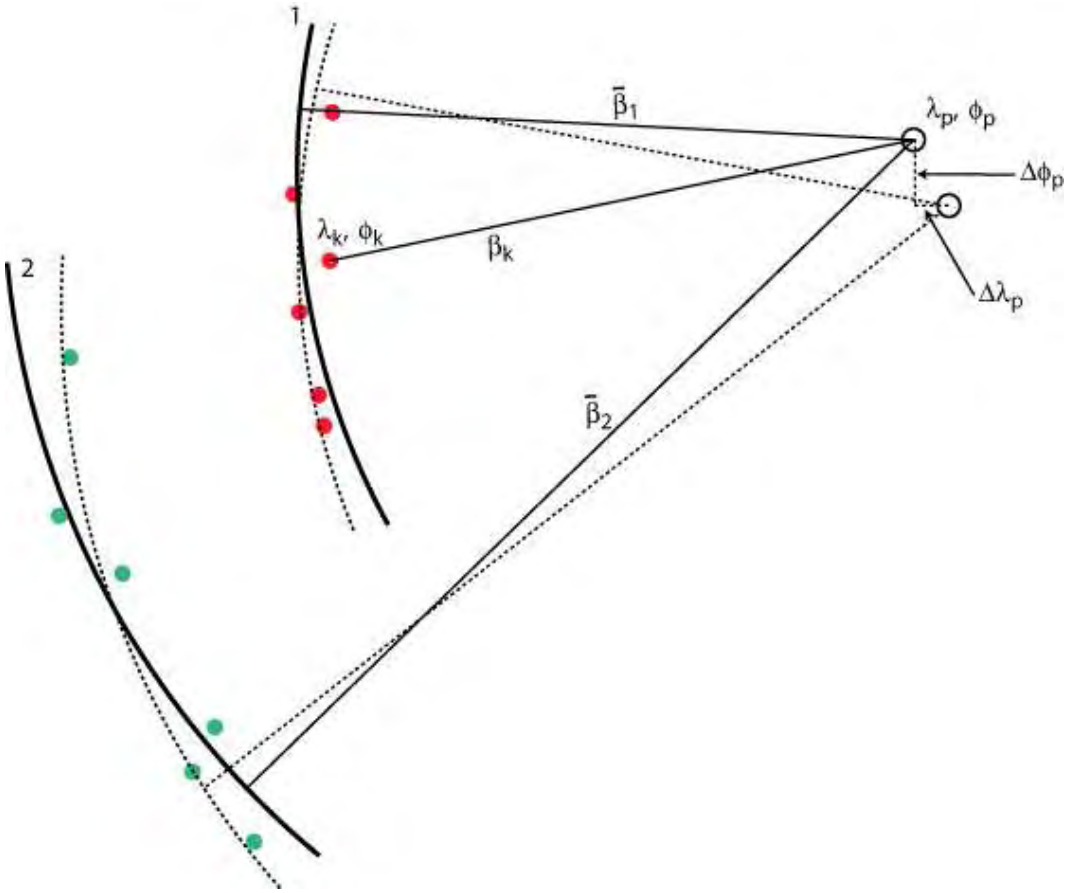

Figure 4.3: Least squares technique for determining stage pole locations. The pole is chosen to minimize the sum of squared distance between the local small circle (lines 1 and 2) and the seamounts (red and green dots)

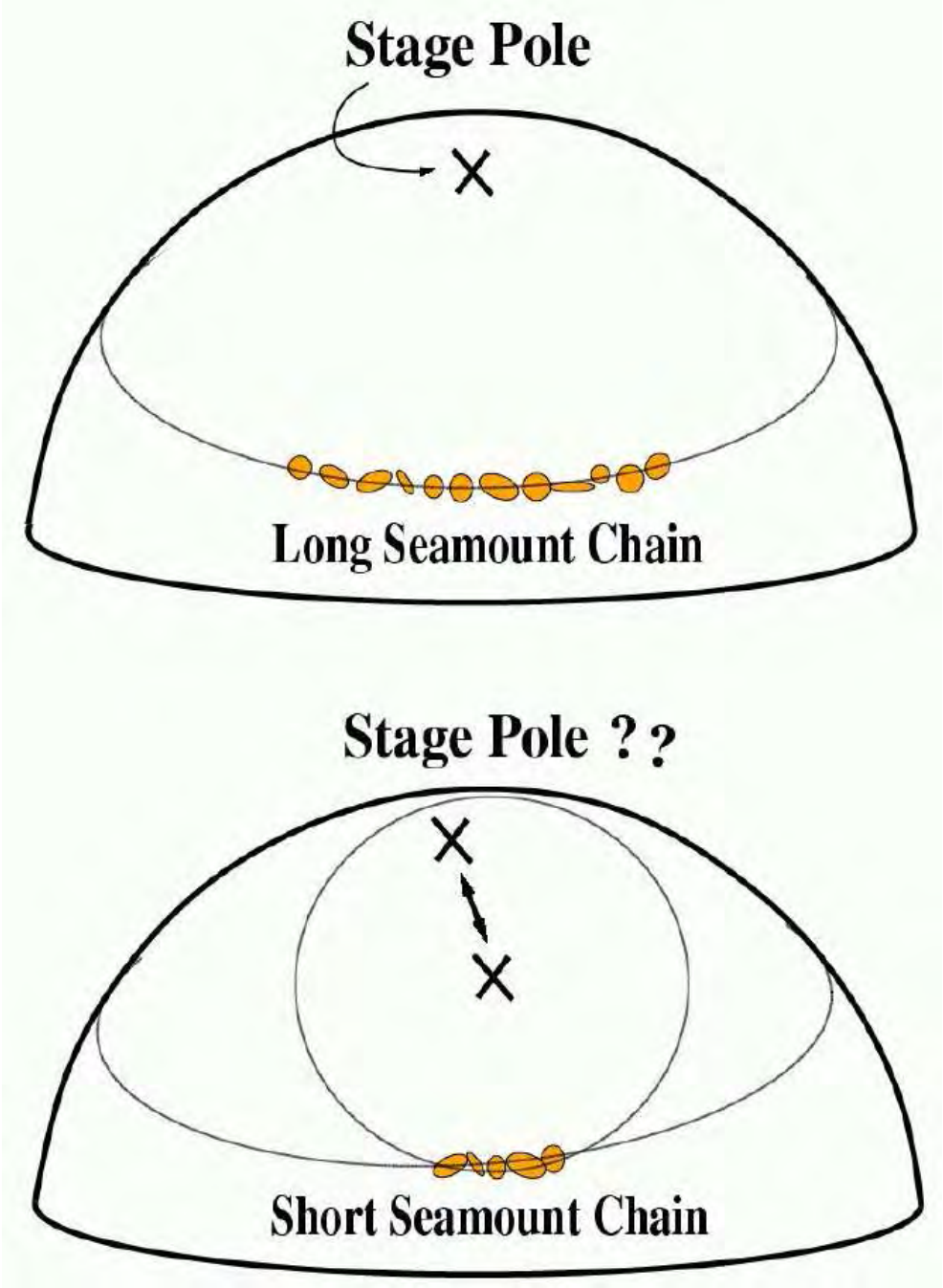

Figure 4.4: Uncertainties associated with fitting small circles to stages. With shorter stages many more pole locations are possible. Figure taken from Harada [1997].

tated with respect to the latter. Determining the finite rotation that moves these seamounts back to their respective hotspot yields one component of a comprehensive APM. The 30 Ma age of these seamounts is just used to explain the concept, in practice no age data is used except 0 Ma which of course is the location of the presently active hotspots. Instead of using age, the search for congruent polygons is carried out using opening angles. Once defined, this polygon can be used to determine absolute plate motions by rotating it just as described above for a lithospheric plate.

4.6 Hotspotting

As previously mentioned in Section 2.7, not all hotspots are as robust as the Hawaiian hotspot. Many have been active for far less time and have delivered a less consistent flux of magma to the surface. Many mantle plumes are active for only a short period of geologic time and then become extinct. Without a presently active volcano to use as a zero age point, using these incomplete hotspot trails to determine absolute plate motions becomes exceedingly difficult. In short, a model of APM cannot be independent from the zero age starting points used to construct that model. Wessel and Kroenke [1997] have developed a geometric technique for determining zero age locations of hotspot trails termed 'hotspotting'. Backtracking of seamounts requires that the seamount first be dated, then using an APM model to move the seamount to its hotspot origin. The path that results from backtracking delineates the expected area of volcanism produced by the hotspot (i.e., the locus of all the younger seamounts produced by that hotspot). It is a common misconception that

the seamount reached its present position by moving along this path. In fact, the seamount riding on the plate has actually taken a far different path from its origin at the hotspot to its present day location. The path the seamount has taken over the mantle has been defined as a seafloor flowline [Wessel and Kroenke, 1998]. The red lines in Figure 4.5 are the flowlines for Detroit, Nintoku and Koko seamounts. Note that the three lines intersect at the hotspot. These paths are of interest because if the hotspot is stationary the hotspot will lie somewhere along these paths. In practice, if we calculate the flowlines for all seamounts in a hotspot chain their flowlines will intersect at the hotspot, provided the APM model is correct and the hotspots are fixed. Instead of using these flowlines and intersections simply as a lines and points we can use seamounts of finite radius and height. Convolving each seamount's bathymetric or gravimetric expression with its flowline produces an elongated ridge of finite width and height. These ridges then intersect at the hotspot and combine to create a local maximum. The sum of these ridges results in a surface which Wessel and Kroenke [1997] termed cumulative volcano amplitude (CVA). The CVA therefore represents cumulative volume of material produced at the hotspot. Wessel and Kroenke [1997] refer to the technique of finding hotspots via CVA maxima as 'hotspotting'. This method does not require a date for the seamount as backtracking does; it only requires an APM model.

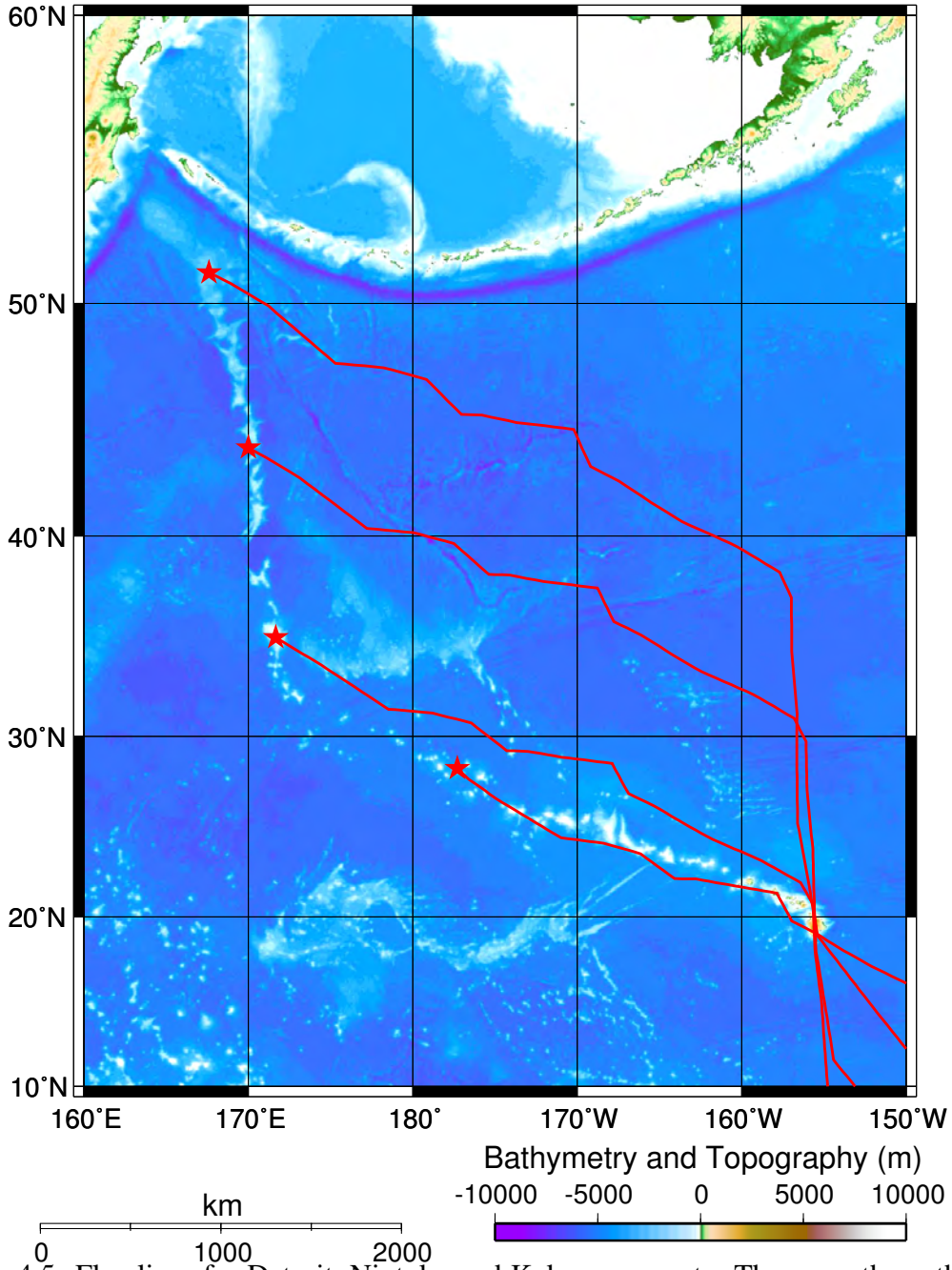

Figure 4.5: Flowlines for Detroit, Nintoku and Koko seamounts. These are the paths that these seamounts traveled over the mantle from their origin at the hotspot to their present locations. If the hotspot is fixed with respect to the mantle, the Pacific plate is rigid and our APM model is correct these flowlines will intersect at the hotspot.

4.7 Modeling Procedure

The first step in the modeling procedure is to define the polygon by assigning a longitude and latitude for the present hotspot location of each hotspot trail to be used. Table 4.1 is a list of initial hotspot locations that define the polygon. The next step is to define a separate envelope for each trail that encompasses all of the hotspot-produced seamounts along each trail. This envelope is based upon bathymetry derived from satellite altimetry [Smith and Sandwell, 1997] and is envelope is used to isolate hotspot-produced seamounts and to exclude other seafloor features that are not associated with the hotspot. If a seamount from a database of Pacific seamounts [Wessel and Lyons, 1997] falls within the envelope the seamount is used in the calculation. This is an improvement upon the technique used by Harada and Hamano [2000] because they used generous envelopes rather than actual bathymetric data or the seamount database. Next, a grid search technique is used to explore all possible rotation pole locations from 180^0 W to 180^0 E longitude and 90^0 N to 90^0 S latitude, with a 5 minute spacing, and all rotation angles from 0-45^0, with a 0.2^0 interval. All of the present hotpot locations that define the polygon are rotated. If the vertice of the rotated polygon falls on top of a seamount belonging to that trail then the rotation is considered successful for that chain. For a rotation to be considered successful overall, in the older part of the model ($\sim$65-12 Ma) it had to fit at least two chains, the Hawaiian-Emperor and Louisville. For the younger portion of the model ($\sim$12-0 Ma) at least two out of three chains including the Hawaiian-Emperor and Louisville and Caroline must be fit. This was done because the Louisville trail has very few young seamounts. This also forces

the model to match younger trails instead of just the Hawaiian-Emperor and the Louisville.

Then, all sucessful poles were then smoothed with a 2^0 filter width to produce a single, representative mean pole for each opening angle; the blue dots and lines in Figure 4.6 show these average poles. Next, we compare cumulative opening angles with observed radiometric ages from Pacific hotspot trails and then fit a linear spline which yields the desired temporal relationship required for an APM model. Finally, we can use the hotspotting technique to determine CVA maxima for each Pacific hotspot trail; these CVA maxima are then used as new and improved hotspot locations that define the polygon for the PFRM. This process was iterated three times.

4.8 Modeling Results

The product of this modeling procedure is a comprehensive model of Pacific absolute plate motion in the hotspot reference frame from 65 Ma to the present. Figure 4.6 shows a plot of finite rotation opening angles plotted against all possible rotation poles and a plot of rotation pole longitude vs. latitude. The color scale is a standard hot scale with white being the highest count and yellow and red fall in the middle and grey represents a zero count. Note that for very small opening angles nearly any pole will work and for large opening angles very few poles will work. Figure 4.7) shows a comparison of cumulative opening angles with observed radiometric ages from Pacific hotspot trails. The optimal linear spline yields stage timing for the model. Table 4.2 shows the pole locations, opening angles and stage timing for the final APM model. Figure 4.8 shows Pacific hotspot trails with the new

APM model overlayed. This APM model fits most Cenozoic hotspot-produced seamount trails on the Pacific plate very well, both geometricaly and chronologicaly. Another result is refined locations for Pacific hotspots based upon the geometry of the Pacific hotspot trails as a group (see Tables 4.3).

Table 4.1: Initial hotspot locations

Hotspot name	Abbreviation	Longitude	Latitude
Hawaiian-Emperor	HI	155.30 W	19.20 N
Louisville	LV	139.00 W	52.50 S
Cobb	CB	130.06 W	45.93 N
Caroline	CR	163.65 E	4.80 N
Marquesas	MQ	138.10 W	10.80 S
Pitcairn	PC	129.40 W	25.63 S
Foundation	FD	111.50 W	38.20 S
Kodiak	KO	131.00 W	50.10 N
Bowie	BW	135.15 W	52.85 N
Tokelau	TS	144.13 W	21.73 S
Austral-Cook	AN	144.95 W	25.75 S
Society	SO	147.84 W	19.133 S
Samoa	SA	168.75 W	16.00 S
Marshall Gilbert	SW	156.43 W	14.40 S

Table 4.2: Final Pacific APM Model

Pole Lon.	Pole Lat.	Tstart(My)	Tend(My)	Angle(deg)
101.001 W	15.95479 N	64.7088	61.1870	2.1723
109.355 W	8.67393 N	61.1870	56.8197	3.4617
100.636 W	14.79763 N	56.8197	52.5588	3.0006
103.651 W	15.93234 N	52.5588	48.1841	3.3409
96.6238 W	32.90236 N	48.1841	44.7384	2.0217
54.2026 W	55.71819 N	44.7384	38.7230	2.8409
39.6057 W	57.09986 N	38.7230	33.7442	2.3869
65.2099 W	57.61518 N	33.7442	31.4375	1.2128
79.2583 W	50.54774 N	31.4375	28.7943	2.3017
34.6095 W	64.11905 N	28.7943	26.6889	1.7891
90.3026 W	57.20005 N	26.6889	23.6257	2.6430
35.6585 W	65.43858 N	23.6257	22.1953	1.2079
42.8779 W	75.92074 N	22.1953	19.2747	2.4651
135.946 W	76.36899 N	19.2747	17.4688	1.6391
79.7634 W	55.72491 N	17.4688	14.6313	2.4298
1.09459 E	69.83531 N	14.6313	11.7381	2.6098
66.5118 W	69.61360 N	11.7381	9.8213	1.6044
73.7013 W	69.23940 N	9.8213	6.8822	2.4807
87.354 W	66.09126 N	6.8822	4.0927	2.4532
53.3567 W	56.17422 N	4.0927	1.6587	2.0550
42.7683 W	40.76116 N	1.6587	0.0010	1.3753

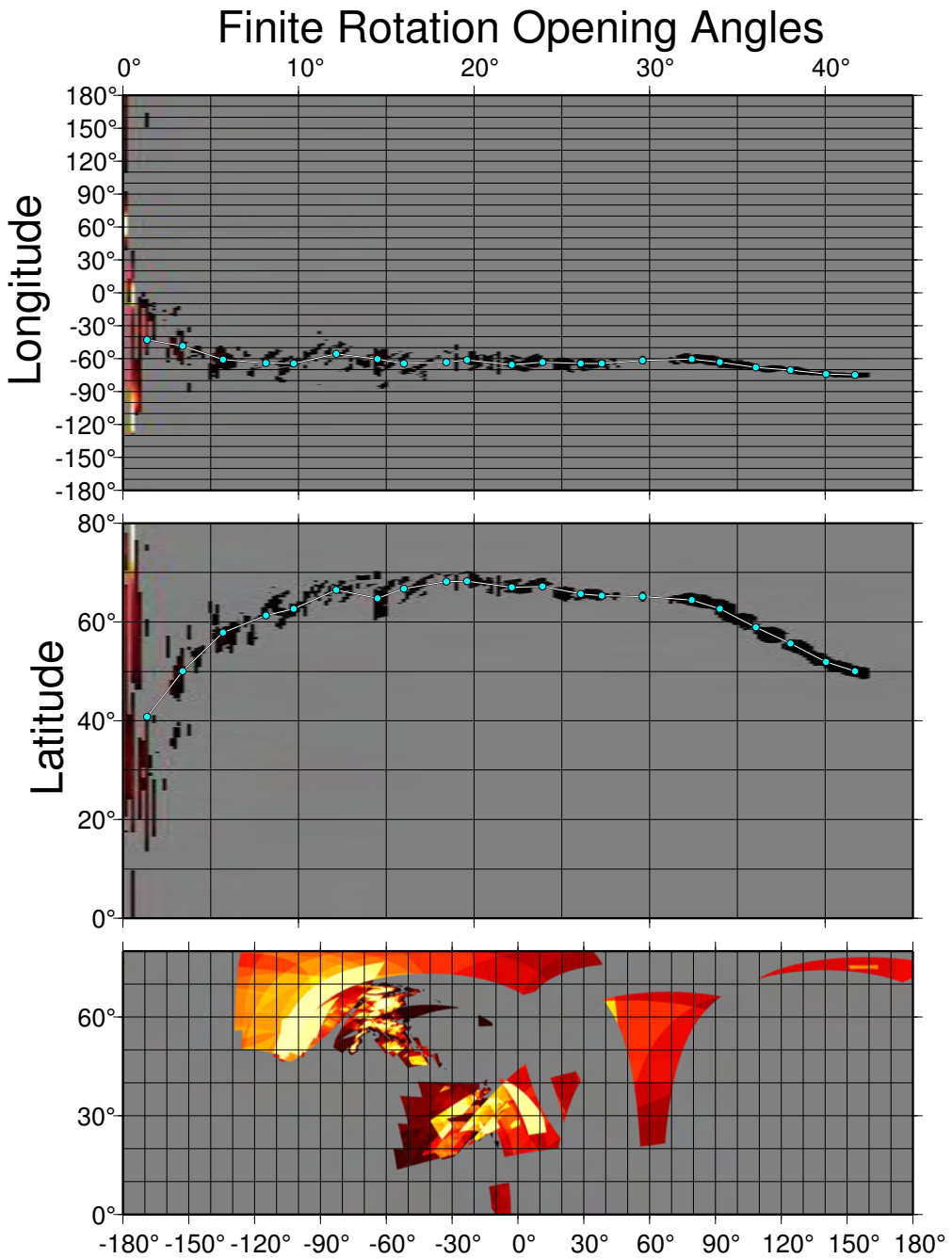

Figure 4.6: The top two plots compare longitude and latitude of rotation poles versus finite rotation opening angles, respectively. The line and blue dots are the final filtered pole locations. The lower plot shows pole location longitude versus latitude.

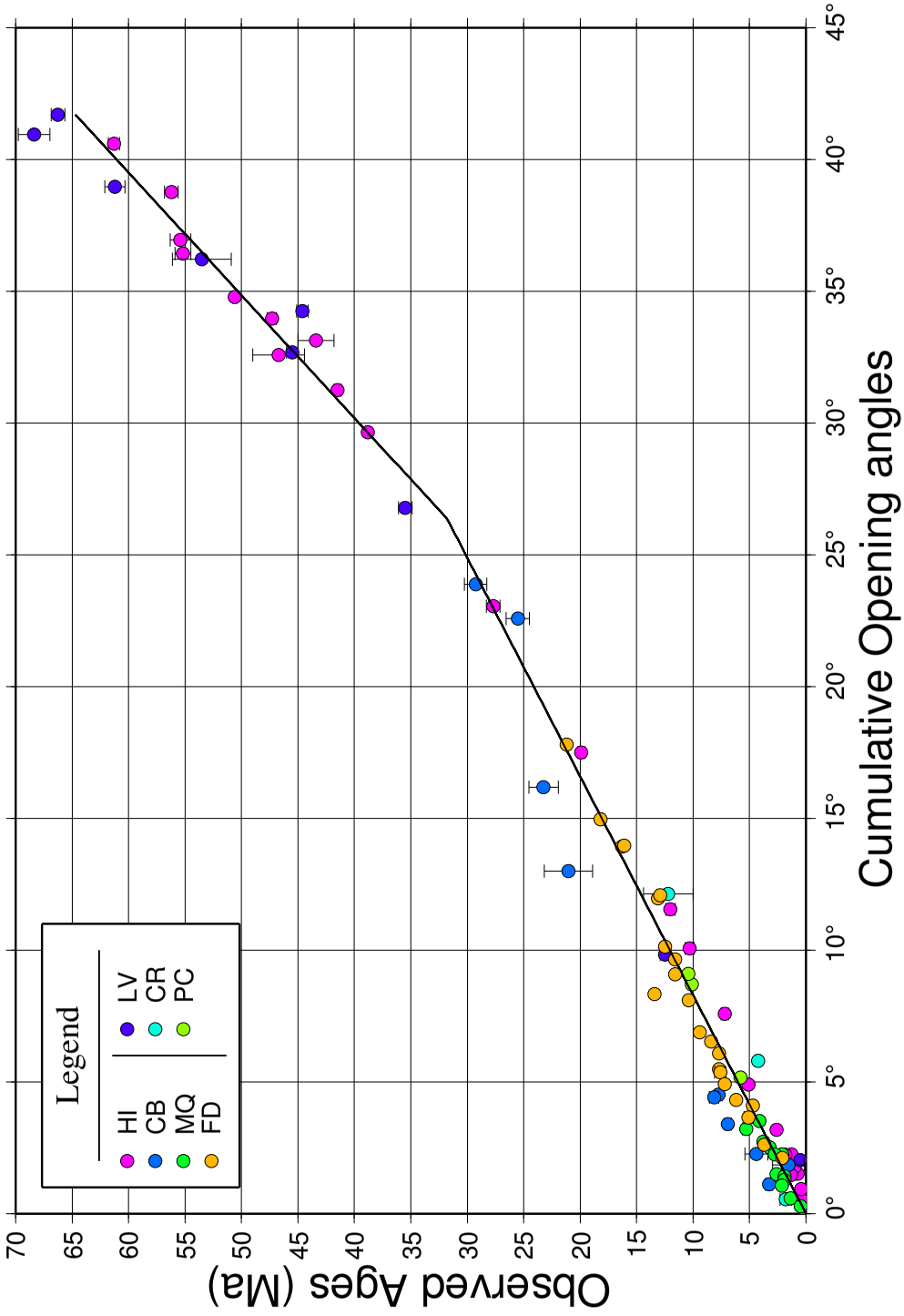

Figure 4.7: Plot of cumulative opening angle versus observed radiometric ages with error bars for Pacific seamounts.

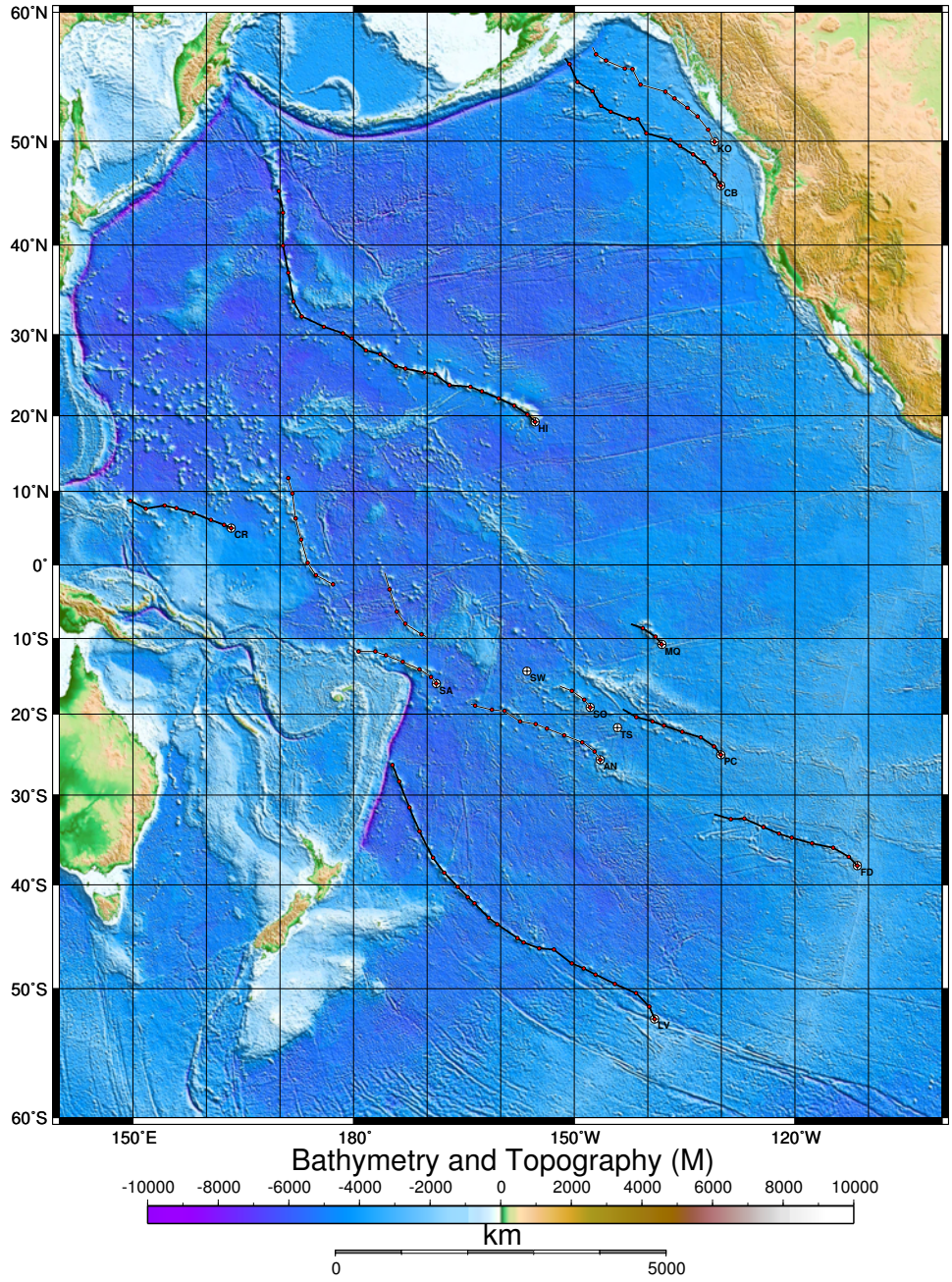

Figure 4.8: Pacific APM model; seamount chains that were used in the modeling procedure are marked by bold lines. Trails that were not used in the modeling procedure are marked by double lines. White dots with crosses are the hotspot locations.

Table 4.3: Final hotspot locations

Hotspot name	Abbreviation	Longitude	Latitude
Hawaiian-Emperor	HI	155.30 W	19.20 N
Louisville	LV	139.06 W	52.56 S
Cobb	CB	130.06 W	45.93 N
Caroline	CR	163.36 E	5.03 N
Marquesas	MQ	138.10 W	10.80 S
Pitcairn	PC	130.06 W	25.13 S
Foundation	FD	111.50 W	38.0 S
Kodiak	KO	131.00 W	50.10 N
Bowie	BW	135.15 W	52.85 N
Tokelau	TS	144.13 W	21.73 S
Austral-Cook	AN	144.95 W	25.75 S
Society	SO	147.84 W	19.133 S
Samoa	SA	168.75 W	16.00 S
Marshall Gilbert	SW	156.43 W	14.40 S

Chapter 5

Correlation of Absolute Plate Motion Changes and Tectonic Events

The model of Pacific Absolute Plate Motion presented here shows several distinct changes in Pacific plate motion. These changes in plate motion create bends in the linear trend of hotspot trails. Evidence of these changes can also be seen in the geologic record throughout the Pacific Rim. Many different dating techniques have been used by many different researchers that are referred to in the following section. A simple literature search for events that match the sense of motion and rough timing of changes in the APM model has been done. The timing may not be exact in many cases but these events do seem to be connected with changes in Pacific APM. The following sections will discuss some possible causes and effects of these changes in Pacific APM.

5.1 48 Ma, The Hawaiian-Emperor Bend

The Hawaiian-Emperor Bend (HEB) has long been considered to be the perfect example of a change in plate motion. Seamounts near the HEB were originally radiometrically dated at ∼43 Ma [Clague and Jarrard, 1973]. Recently, rock samples from the bend were redated and found to be much older than previously thought. Kimmei and Daikakuji seamounts, which are located at the HEB have been redated at ∼47 Ma [Sharp and Clague, 1999, 2002]. These researchers suggest an age of ∼50 Ma for the bend. The rocks dated from these seamounts are post-shield transitional to alkalic basalts and trachytes. If these rocks are from the alkalic cap stage rather than the post-erosional stage it would be reasonable to suggest that the start of the shield building stage would have began approximately 1-2 million years earlier rather than the 3 million years suggested by [Sharp and Clague, 1999, 2002]. A better estimate of the timing of the HEB may be ∼48-49 Ma or ∼Chron 21-22.

The HEB is the clearest change in the trend of a hotpost trail on the planet. If this was truly the result of a large change in plate motion we would also expect to see changes in RPM between the Pacific and neighboring plates, as well as major changes in the tectonic regimes around the Pacific plate. Norton [1995] concluded that there were no significant tectonic events around the Pacific to suggest a change in plate motion at 43 Ma. With a new age of ∼48-49 Ma we can correlate many tectonic events and RPM changes around the Pacific with the change in absolute plate motion that would have created the HEB.

A change in plate motion as large as the 48 Ma event would create widespread changes in the tectonic and volcanic regimes of the Pacific and neighboring plates; indeed this is

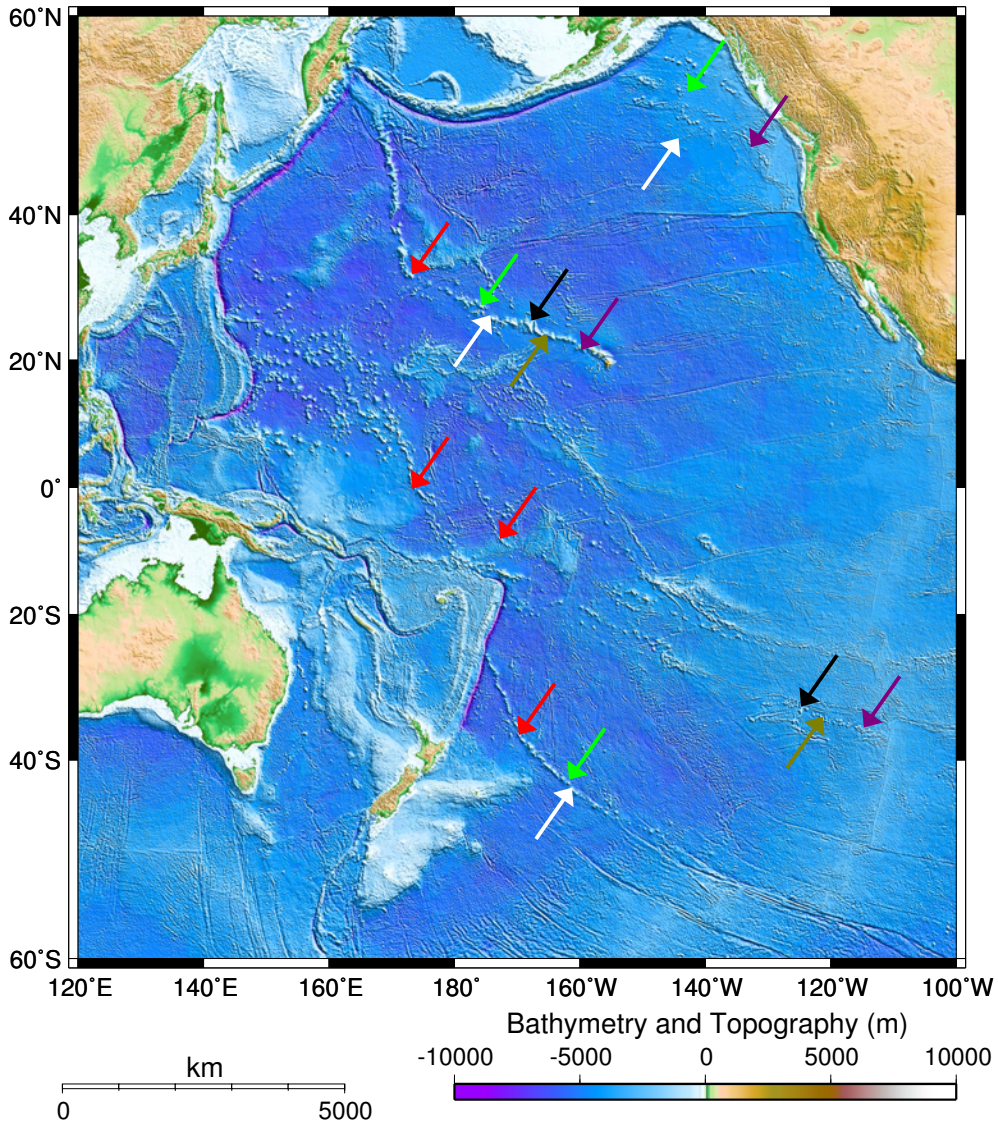

Figure 5.1: Arrows point to locations of kinks in Pacific hotspot trails produced by changes in Pacific APM (red = 48 Ma, green = 27 Ma, white = 23 Ma, black = 18, tan = 12, and purple = 6 Ma).

the case. Figure 5.2 shows APM vectors before and after the change in plate motion as well as differential motion vectors (see Table 4.2 for rotation parameters). In the South Pacific major triple junction reorganizations began as Pacific-Antarctic spreading propagated northward to intersect the Pacific-Farallon Ridge. Spreading ended at the Pacific-Aluk Ridge at ∼Chron21, leaving the Henry and Hudson Troughs as tectonic scars. Further south in the Ross Sea, motion between East and West Antartica began at ∼Chron 20o in the Adare Trough [Cande et al., 2000]. The spreading rate increased between Australia and Antarctica at Chron 21y [Tikku and Cande, 1999]. In the southwest Pacific subduction was initiated along the Manus-North Solomon-Vitiaz (Melanesian) Trench [Kroenke, 1984]. The most significant event occured in the western Pacific, the formation of the Izu-Bonin-Mariana (IBM) subduction system is thought to have begun at approximately 49 Ma or perhaps as early as 52 Ma, evidenced by the emplacement of boninites in the forearc [Cosca et al., 1998]. In the North Pacific major changes were occuring along the Aleutian Subduction Zone. As the subduction zone began to accommodate dextral slip at its western end, Aleutian volcanic activity waned between 45 and 40 Ma. In the Northeast Pacific major spreading reorganization began before the HEB event. The Vancouver plate split from the Farallon plate at this time followed by stable spreading which began at Chron 21 [Atwater and Stock, 1998].

Another interesting observation is that the volume of material produced by the Hawaiian hotspot decreased significantly after the bend: seamounts just east of the HEB are smaller and spaced further apart than those immediately before the HEB. Output from the hotspot was back to normal by about 34 Ma. Several other Pacific hotspot trails also appear to have

bends produced by this change in Pacific APM (see Figure 5.1).

The Louisville seamount chain has a less pronounced bend than the HEB but it is still recognizable. At the southern ends of the Marshall-Gilbert ridge and the Tokelau island group there also appear to be bends coeval with the HEB. However, there is limited age data available to confirm what appears to be implied by the geometry. It is also worthwhile to note that these trails either die out or drastically reduce their output similar to Hawaii just after these bends. The Easter-Line trail also appears to change azimuth in the vicinity of the Tuamotu plateau around this time. There are very few radiometric dates from these trails but the few available dates, and certainly the geometry, strongly suggest that there was a large change in the direction and velocity of the Pacific Plate at $\sim$48 Ma.

5.2 27-23 Ma

At 27 Ma the Pacific Plate once again began to change direction and move towards the north. For approximately 4 million years the plate continued to move in this direction, then at about 23 Ma it resumed movement towards the west. Several hotspot-produced seamount trails on the Pacific plate reflect this change in their geometry, which roughly appears as a north-to-south jog. Lonsdale [1988] noted a small offset in the Louisville chain near 161.5^0W and speculated that it was coeval with a prominent offset seen in the Hawaiian chain near 175^0W. Wessel and Kroenke [1998] have proposed that the Cobb seamount trail may also contain yet another coeval offset. In the western Pacific at approximately 27 Ma the newly formed young buoyant crust of the Caroline Basin [Hegarty et al., 1982] collided

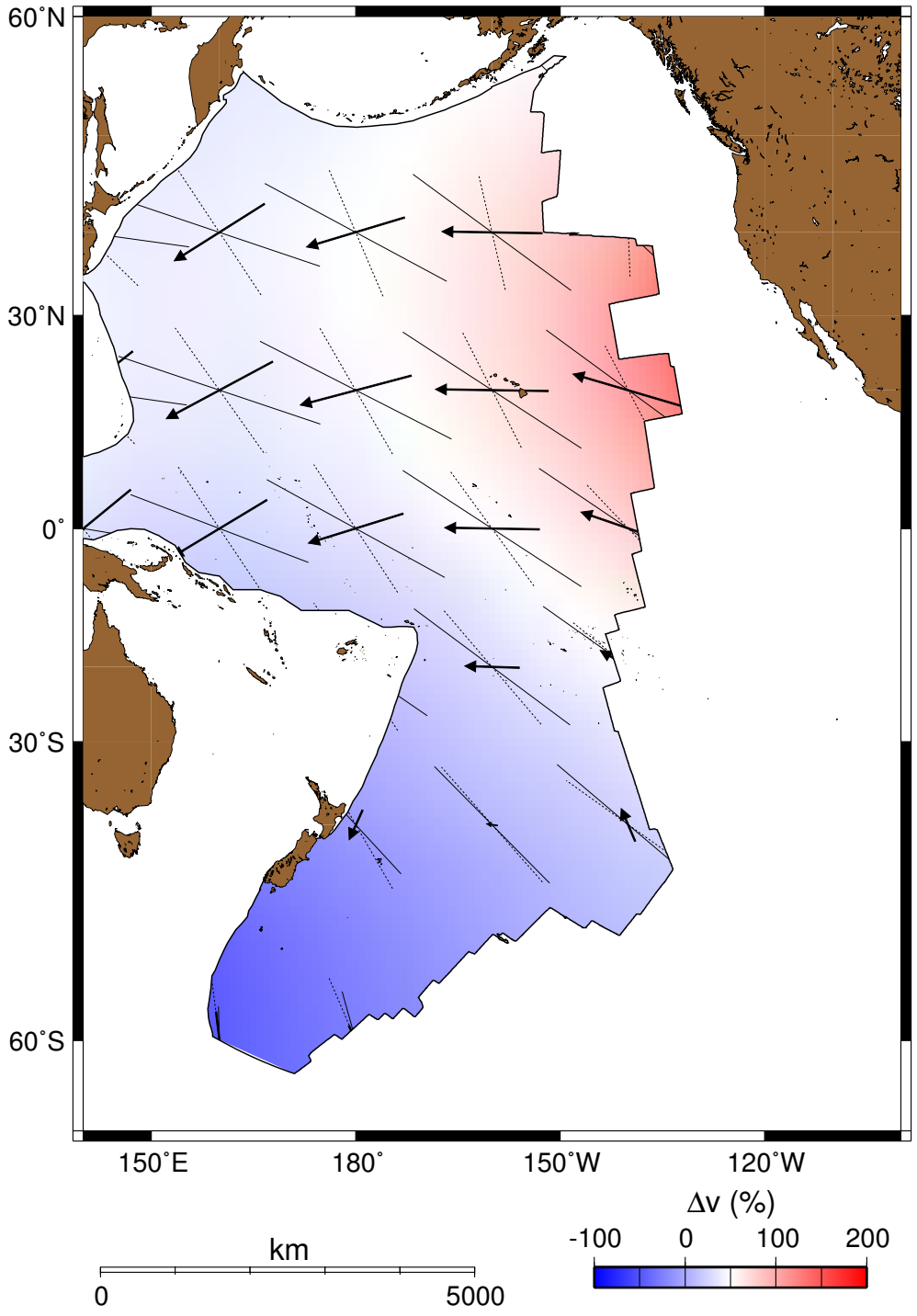

Figure 5.2: Change in Pacific APM at 48 Ma. Solid lines are APM vectors after 48 Ma, dotted lines are APM vectors before 48 Ma and solid arrows are differential motion vectors at 48 Ma

with the Manus Arc. The result of this collision was to halt subduction along the Melanesian Trench [Petterson et al., 1997], which in turn caused the Pacific plate to be forced northward by the Australian plate. The northward movement of the Pacific and Australian plates generated changes in the tectonic regime throughout the Pacific Basin. Figure 5.3 and Figure 5.4 shows APM vectors before and after the 27 and 23 Ma changes in plate motion as well as differential motion vectors at the time of the change (see Table 4.2 for rotation parameters). In the western Pacific, the Caroline ridge spreading system died. The Parece Vela Ridge was then pushed to the north, changing the relative motion of spreading in the Parece Vela Basin. The result of this change in relative plate motion was the formation of S-shaped fracture zones in the Parece Vela Basin [Okino et al., 1998, 1999]. In the Northeast Pacific there is also evidence of this northward jog in Pacific plate motion. Subduction beneath the Wrangell Mountains began around 27 Ma, and arc volcanism followed beginning at 26-25 Ma [Richter et al., 1990].

In the eastern Pacific, a major tectonic reorganization was occurring. In the late Oligocene at 28.5 Ma, the eastward migrating EPR collided with the North American Continent and began to subduct beneath it [Atwater, 1970] and eventually evolved into the San Andreas transform system [Crowell, 1979]. Also Dilles and Gans [1995] conclude that faulting began in the southern Basin and Range province between 26 and 24.7 Ma. Further south, the Farallon plate split into the Cocos and Nazca plates around 26 Ma [Handschumacher, 1976; Hey, 1977; Lonsdale and Klitgord, 1978]. South of the Agassiz fracture zone in the southeast Pacific, westward migration of the East Pacific Ridge and the Pacific Antarctic Ridge occurred relative to the Chile Ridge, as northward ridge propagation initi-

ated north of the Agassiz Fracture Zone [Tebbens and Cande, 1997; Tebbens et al., 1997]. The trends of the Heezen, Tharp and Tula fracture zones have an abrupt 12-degree change near the beginning of anomaly 7 (26 Ma). New fracture zones were also created south of the Udintsev fracture zone and within the Eltanin fault system [Lonsdale, 1986]. Lonsdale [1988] suggests that these changes in Pacific-Antarctic relative plate motion were the result of a change in the velocity of the fast moving Pacific plate rather than a change in motion of the slow moving Antarctic plate. In the southwest Pacific, subduction began along the Tonga Trench, with Tonga (Lau-Colville) Arc volcanism beginning at approximately 25 Ma [Kroenke, 1984]. Stratigraphic and structural changes dated in New Zealand also indicate that the modern Pacific-Australian plate boundary including the Hikurangi Trench and the Alpine Fault formed between 28 and 24 Ma [Kamp, 1991]. Back-arc spreading ended in the South Fiji Basin immediately north of New Zealand at 26.5 Ma [Malahoff et al., 1982]. Spreading south of New Zealand on the easternmost portion of the Southeast Indian Ridge also ended at this time [Williamson, 1974; Kamp, 1986].

5.3 18-12 Ma

The next major change in Pacific plate motion occurred around 18 Ma. At this time the Pacific plate once again began to move in a more northerly direction. This change in plate motion was similar to the 27-23 Ma event in direction and also appears to have lasted for about 4 to 6 my and then the Pacific plate resumed motion towards the west. An offset produced by this change in plate motion can be seen in the Hawaiian chain at 168^0W. A

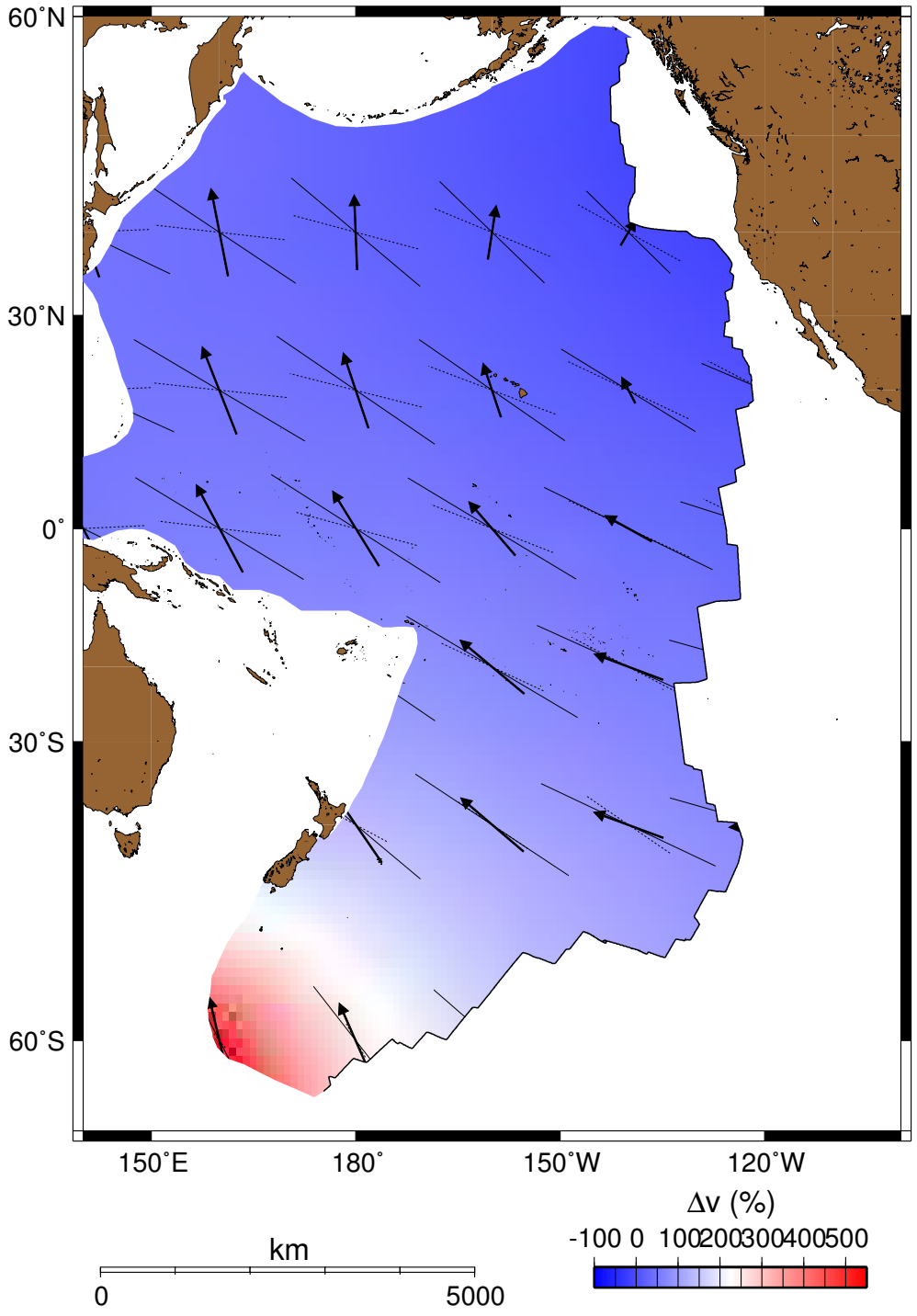

Figure 5.3: Change in Pacific APM at 27 Ma. Dotted lines are APM vectors before 27 Ma, solid lines are APM vectors after 27 Ma and solid arrows are differential motion vectors at 27 Ma

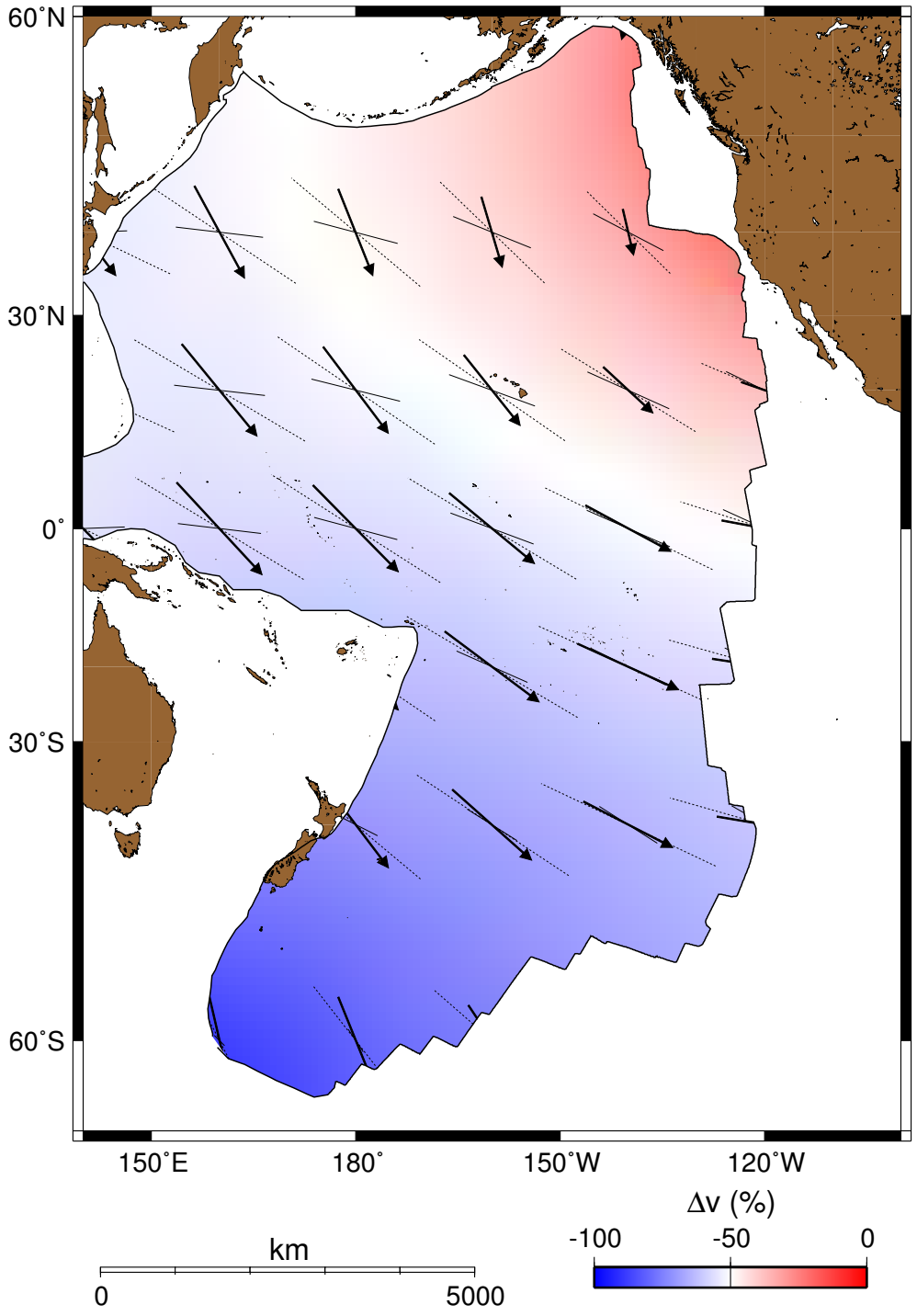

Figure 5.4: Change in Pacific APM at 23 Ma. Dotted lines are APM vectors before 23 Ma, solid lines are APM vectors after 23 Ma and solid arrows are differential motion vectors at 23 Ma

similar offset was also produced in the Foundation chain at 122^0W. Offsets in the Caroline and Cobb trails are also present. The impact of this change in Pacific APM was once again Pacific-wide. Figure 5.5 and Figure 5.6 shows APM vectors before and after the changes in plate motion at 18 and 12 Ma as well as differential motion vectors at the time of the change (see Table 4.2 for rotation parameters). In the western Pacific arc volcanism was briefly rejuvenated along the Melanesian Arc and extension occured along the Maramuni Arc [Hill and Raza, 1999]. In the southeastern Pacific at 18-16 Ma, Chile Ridge-Trench collisions [Tebbens et al., 1997] caused the spreading rate to slow along the Chile Ridge. The Agassiz-Valdivia fracture zones began to separate as northward ridge propagation was initiated north of the Valdivia Fracture Zone, forming the North Chile Ridge [Tebbens and Cande, 1997]. In the eastern Pacific, a change in relative motion between the Pacific and North American plates occured. Zoback et al. [1994] concluded that "The interval between 17 and 14 Ma was a dynamic period in parts of Nevada, Oregon, Idaho and Washington". In the Basin and Range province rapid extension occured Dilles and Gans [1995]. Prior to 15 Ma there was no extensional faulting southeast of Walker Lane, then volcanism and east-west extension of greater than 150% occured between 13.8 and 12.6 Ma. In the eastern Basin and Range Province rapid slip of 12-15 km along the Snake Range-Deep Range Creek Range fault system in east-central Nevada, with domal uplift of gneiss domes. Ingersoll and Rumelhart [1999] propose a three stage model for the evolution of the Los Angeles Basin beginning with a period of transrotation between 18-12 Ma.

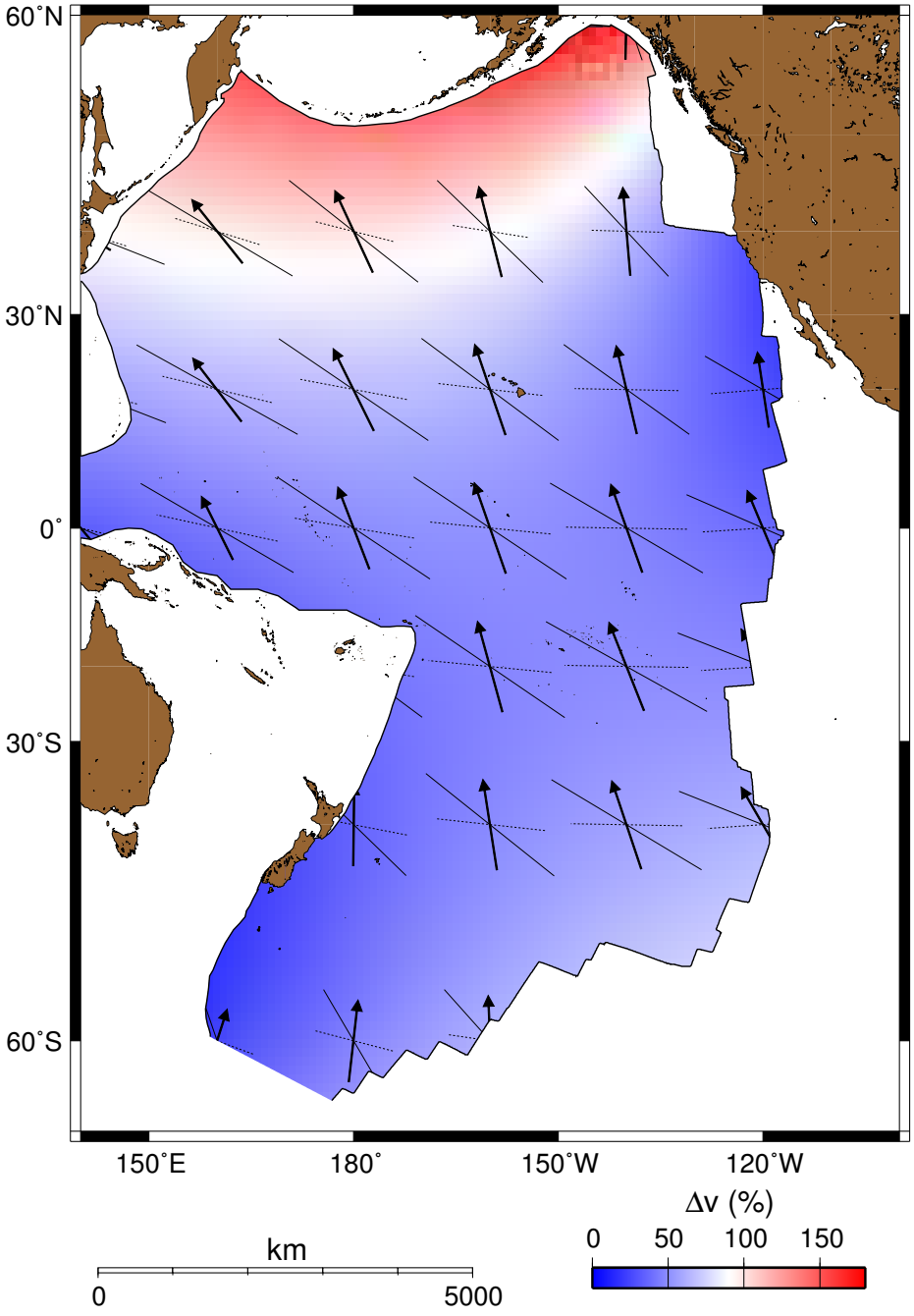

Figure 5.5: Change in Pacific APM at 18 Ma. Dotted lines are APM vectors before 18 Ma, solid lines are APM vectors after 18 Ma and solid arrows are differential motion vectors at 18 Ma

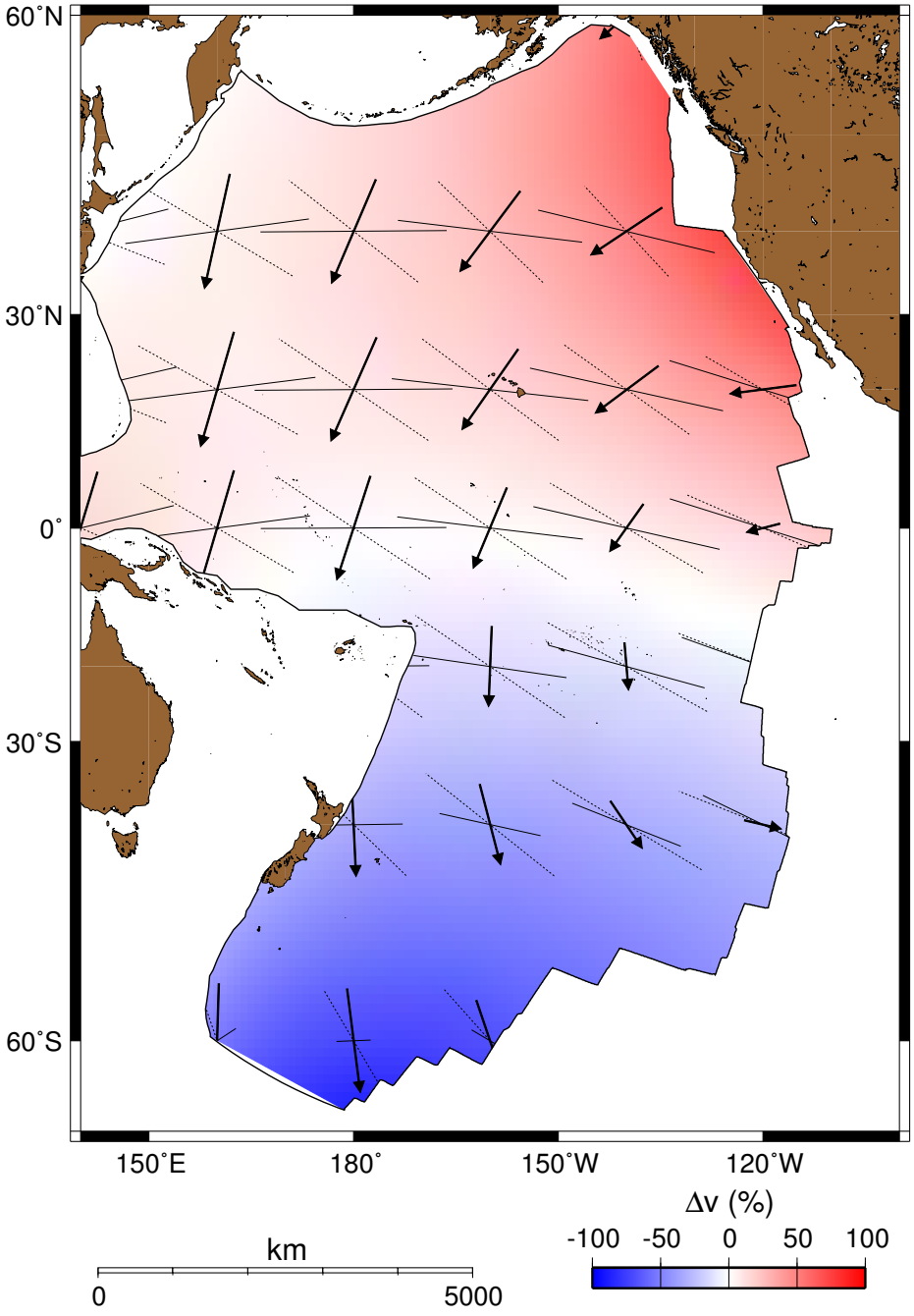

Figure 5.6: Change in Pacific APM at 12 Ma. Dotted lines are APM vectors before 12 Ma, solid lines are APM vectors after 12 Ma and solid arrows are differential motion vectors at 12 Ma

5.4 6 Ma

At 6 Ma another large change in Pacific plate motion began. With a pattern similar to older events, this change also produced an offset towards the south in the Hawaiian chain in the vicinity of the island of Kauai. The Foundation, Cobb and Marquesas chains also reflect this change in their geometry. The circum-Pacific tectonic events associated with this change are also impressive. Figure 5.7 shows APM vectors before and after the change in plate motion as well as differential motion vectors (see Table 4.2 for rotation parameters). The spreading rate slowed along the Chile Ridge [Tebbens et al., 1997]. In the western Pacific rapid tectonic uplift in Malaita located on the southern side of the Ontong Java Plateau began at approximately 6 Ma, increased between 4 and 2 Ma and continues today [Neal et al., 1997; Petterson et al., 1997]. Compressional seismicity east of the plateau [Okal et al., 1986] and seafloor structural deformation [Kroenke and Walker, 1986] suggest crustal shortening. Seafloor spreading began in the Woodlark Basin at $\sim$6 Ma and in the Manus Basin at 3.5 Ma [Taylor, 1979; Taylor et al., 1995]. On the Caroline plate spreading began in the Sorol trough and subduction began along the Mussau trench [Hegarty et al., 1982]. The Aleutian arc began to be broken into several rotating blocks beginning at 6 Ma [Geist et al., 1988]. In the eastern Pacific the southern San Andreas fault became active as the Baja Peninsula was tranferred to the Pacific plate when spreading began in the Gulf of California. The cause of this change in Pacific APM appears to be a complex interaction between the northern margin of the Australian plate and the adjacent Ontong Java Plateau located on the Pacific plate. The OJP is a massive oceanic plateau formed

in the Cretaceous by rapid voluminous eruption of basaltic magma onto the seafloor. The OJP is approximately the size of Greenland and it covers an area of 1.5x $10^6 km^2$ with crustal thickness in the 35-45 km range [Neal et al., 1997]. The buoyant plateau is not a likely candidate for subduction [Cloos, 1993]; instead it appears to have clogged up the subduction zone and caused the widespread deformation discussed earlier. It appears that the collision of OJP with the northern margin of the Australian plate intensified around 6 Ma.

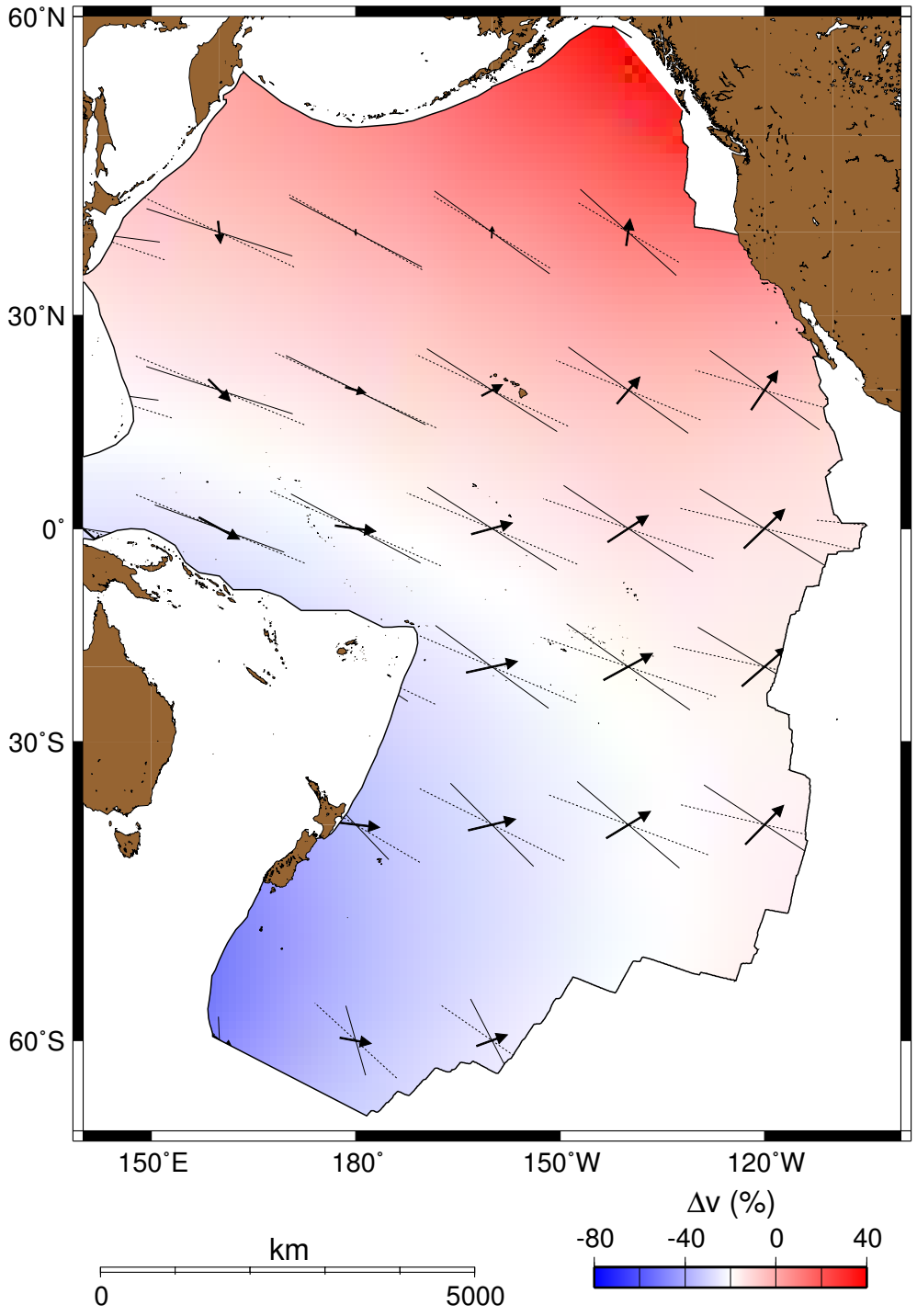

Figure 5.7: Change in Pacific APM at 6 Ma. Dotted lines are APM vectors before 6 Ma, solid lines are APM vectors after 6 Ma and solid arrows are differential motion vectors at 6 Ma

Chapter 6

Discussion and Conclusions

The model presented here is far from perfect, allthough it is the most geometrically accurate model of Pacific APM yet created. The offsets seen in Pacific hotspot trails must be the result of a change in APM, hotspot drift or channeling of magma due to pre-existing features in the lithosphere. The sense of motion inferred from these kinks appears to correlate well with the sense of motion and the timing of the circum Pacific tectonic events discussed. Much more research is required to better constrain this and other models. In particular a paleomagnetic test of the Louisville Seamount Chain, similar to the one done on the Hawaii-Emperor Seamount Chain would be valuable. Additional radiometric dates from Pacific seamounts would also be useful.

The modeling procedure used is still in the development stage. A more robust technique may be necessary to accommodate the large number of variables associated with the modeling procedure. A major problem arises when trying to pinpoint hotspot locations. Different local minima and maxima tend to be found depending on the initial conditions. A

more advanced technique may be able to determine global minima and maxima. Age data are also a major problem as less then 1% of Pacific seamounts have been dated. Many of the available dates may also be unreliable. The same problem holds for the tectonic events discussed. Numerous events dated by various sources and techniques have been sorted into groups that appear to correlate well with the changes in Pacific APM suggested here.

The results from paleomagnetic tests of hotspot fixidity leave something to be desired. As seen in Figure 3.1 the error bars from the ODP results are large. Also, ODP hole 1204 on Detroit seamount was drilled in "flat basement" similarly hole 1205 was also drilled in flat basement. Subaerial Hawaiian volcanoes generally have slopes of $\sim$5 degrees. Sager and Koppers [2000] have concluded that there was TPW between 79-39 Ma and this could explain the discrepancies in paleolatitiudes. Models of mantle flow are also suspect [Steinberger, 2000; Steinberger and O'Connell, 2000]. Small pertubations to the initial conditions have drastic effects on the final results. The fact remains that we can fit the geometry and geochronology of numerous Pacific hotspot trails with a simple model of Pacific APM based on the assumptions of fixed hotspots and rigid plates. There seems to be no need to invoke hotspot drift.

With the assumptions of fixed hotspots and rigid plates I have created a model of Pacific absolute plate motion. This model fits known Pacific hotspot trails well, both chonologically and geometrically. Large changes in Pacific absolute plate motion have occured in the geologic past at approximately 48, 27, 23, 18, 12 and 6 Ma; these changes in plate motion are recorded as kinks in the linear trends of Pacific hotspot trails. The timing of these large scale changes in plate motion also appear to correlate with Pacific-wide tectonic events.

These changes in APM can happen rapidly (1-2 my). Subduction may be the major driving mechanism in plate tectonics [Forsyth and Uyeda, 1975], but ending rather than starting subduction may be the main cause of many plate motion changes. The collision of large bouyant geologic features with convergent plate boundaries and the subsequent end to subduction often times appears to be responsible for rapid changes in the motion of large lithospheric plates. My analysis leads to the conclusion that the initial assumptions of fixed hotspots and rigid plates are valid. Pacific hotspots have been stationary with respect to each other over the past 65 My and can provide an absolute reference frame for tectonic analysis.

Bibliography

T. Atwater. Implications of the plate tectonics for the Cenozoic tectonic evolution of western North America. *Geol. Soc. Am. Bull.*, 81:3513–3536, 1970.

T. Atwater and J. Stock. Pacific-North America plate tectonics of the Neogene southwestern united states; an update. *Int. Geol. Rev.*, 40(5):375–402, 1998.

E. T. Baker, C. G. Fox, and Cowen J. P. In situ observations of the onset of hydrothermal discharge during the 1998 submarine eruption of Axial Volcano, Juan de Fuca Ridge. *Geophys. Res. Lett.*, 26(23):3445–3448, 1999.

J. Besse and V. Courtillot. Revised and synthetic Apparent Polar Wander paths of the African, Eurasian, North American and Indian plates, and True Polar Wander since 200 Ma. *J. Geophys. Res.*, 96:4029–4050, 1991.

S. C. Cande, J. M. Stock, R. D. Müller, and T. Ishihara. Cenozoic motion between East and West Antarctica. *Nature*, 404:145–150, 2000.

S.C. Cande, C. A. Raymond, J. Stock, and W. F. Haxby. Geophysics of the Pitman fracture zone and Pacfic-Antarctic plate motions during the Cenozoic. *Science*, 270:947–953, 1995.

D. A. Clague. The growth and subsidence of the Hawaiian-Emperor volcanic chain. In A. Keast and S. E. Miller, editors, *The Origin and Evolution of Pacific Island Biotas*, volume in press, pages 35–50. SPB Acad., Amsterdam, 1996.

D. A. Clague and R. D. Jarrard. Tertiary plate motion deduced from the Hawaiian-Emperor chain. *Geol. Soc. Am. Bull.*, 84:1135–1154, 1973.

M. Cloos. Lithospheric buoyancy and collisional orogenisis; subduction of oceanic plateaus, continental margins, island arcs, spreading ridges, and seamounts. *Geol. Soc. Am. Bull.*, 105(6):715–737, 1993.

M. A. Cosca, R. J. Arculus, J. A. Pearce, and J. G. Mitchell. $^{40}Ar/^{39}Ar$ and K-Ar geochronological age constraints for the inception and early evolution of the Izu-Bonin-Mariana arc system. *The Island Arc*, 7:579–595, 1998.

A. Cox and D. Engebretson. Change in motion of the Pacific plate at 5 Ma BP. *Nature*, 313:472–474, 1985.

R. T. Cox. Hawaiian volcanic propagation and Hawaiian swell asymmetry: evidence of northwestward flow of the deep mantle. *Tectonophysics*, 310:69–79, 1999.

J. C. Crowell. The San Andreas fault system through time. *J. Geol. Soc. London*, 136: 293–302, 1979.

C. W. Devey, R. Hekinian, D. Ackermand, N. Binard, B. Francke, C. Hemond, V. Kapsimalis, S. Lorenc, M. Maia, H. Moller, K. Perrot, J. Pracht, T. Rogers, K. Stattegger, S. Steinke, and P. Victor. The Foundation Seamount Chain: a first survey and sampling. *Marine Geology*, 137:191–200, 1997.

J. H. Dilles and P. B. Gans. The chonology of Cenozoic volcanism and deformation in the Yerington area, Western Basin and Range and Walker Lane. *Geol. Soc. Am. Mem.*, 107 (104):474–486, 1995.

R. Duncan and M. A. Richards. Hotspots, mantle plumes, flood basalts and trus polar wander. *Rev. Geophys.*, 29:31–50, 1991.

R. A. Duncan and D. A. Clague. Pacific plate motion recorded by linear volcanic chains. In A. E. M. Nairn, F. G. Stehli, and S. Uyeda, editors, *The Ocean Basins and Margins*, volume 7A, pages 89–121. Plenum, New York, 1985.

R. A. Duncan, I. McDougall, R. M. Carter, and D. S. Coombs. Pitcairn Island - another Pacific hot spot? *Nature*, 251:679–682, 1974.

D. W. Forsyth and S. Uyeda. On the relative importance of the driving forces of plate motion. *Geophys. J.*, 43:163–200, 1975.

E. L. Geist, J. R. Childs, and D. W. Scholl. The origin of summit basins of the Aleutian ridge: Implications for block rotation of an arc massif. *Tectonics*, 7(2):327–341, 1988.

P. Goldreich and A. Toomre. Some remarks on Polar Wandering. *J. Geophys. Res*, 74: 2555–2567, 1969.

D. W. Handschumacher. Post-Eocene tectonics of the eastern Pacific. In G. H. Sutton, M. H. Manghnaui, and R. Moberly, editors, *The Geophysics of the Pacific Ocean and its Margins*, pages 117–202. American Geophysical Union, 1976.

Y. Harada. New accurate models of the plate motions relative to the hotspots and the cause of the dexcrepancy in the global plate-motion circuit. *EOS Trans. AGU*, 78(46):F721, 1997.

Y. Harada and Y. Hamano. Recent Progress on the Plate Motion Relative to Hotspots. In M. A. Richards, R. G. Gordon, and R. D. van der Hilst, editors, *The History and Dynamics of Global Plate Motions*, volume 121 of *Geophysical Monongraph Series*, pages 327–339. American Geophysical Union, 2000.

K. A. Hegarty, J. K. Weissel, and D. E. Hayes. Convergence at the Caroline-Pacific plate boundary: Collision and subduction. In D. E. Hayes, editor, *The Tectonic and Geologic Evolution of southeast Asian Seas and Islands, part 2, Geophys. Monogr. Ser.*, volume 27, pages 326–348. AGU, Washington, D. C., 1982.

R. Hekinian, P. Stoffers, C. Devey, D. Ackerman, C. Hemond, J. O'Connor, N. Binard, and M. Maia. Intraplate versus ridge volcanism on the Pacific-Antarctic Ridge near $37^0S - 111^0W$. *J. Geophys. Res*, 102:12,265–12,286, 1997.

R. N. Hey. Tectonic evolution of the Cocos-Nazca spreading center. *Geol. Soc. Am. Bull.*, 88:1414–1420, 1977.

K. C. Hill and A. Raza. Arc-continent collision in Papua Guinea: Constraints from fission track thermochronology. *Tectonics*, 18(6):950–966, 1999.

R. V. Ingersoll and P. E. Rumelhart. Three-stage evolution of the Los Angeles basin, southern California. *Geology*, 27(7):593–596, 1999.

H. P. Johnson and M. Helferty. The geological interpretation of side-scan sonar. *Rev. Geophys.*, 28(4):357–380, 1990.

P. J. J. Kamp. Late Cretaceous-Cenozoic tectonic developement of the southwest Pacific region. *Tectonophysics*, 121:225–251, 1986.

P. J. J. Kamp. Late Oligocene Pacific-wide tectonic event. *Terra Nova*, 3:65–69, 1991.

J. L. Karsten and J. R. Delaney. Hot spot-ridge crest convergence in the northeast Pacific. *J. Geophys. Res.*, 94(B1):700–712, 1989.

B. H. Keating, D. P. Mattey, J. J. Naughton, D. Epp, A. Lazarewicz, and D. Schwank. Evidence for a hot-spot origin of the Caroline islands. *J. Geophys. Res.*, 89(B12):9937–9948, 1984.

A. A. P. Koppers, J. P. Morgan, J. W. Morgan, and H. Staudigel. Testing the fixed hotspot hypothesis using ^{40}Ar/^{39}Ar age progressions along seamount trails. *Earth Planet. Sci. Lett.*, 185:237–252, 2001.

L. W. Kroenke. *Cenozoic tectonic development of the southwest Pacific*, volume 6 of *Tech. Bull. – U.N. Econ. Soc. Comm. Asia Pac. Comm. Co-ord. Jt. Prospect Miner. Resour. South Pac. Offshore Areas*. 1984.

L. W. Kroenke and D. A. Walker. Evidence for the formation of a new trench in the western Pacific. *EOS Trans. AGU*, 67(12):145–146, 1986.

M. Kurz. Personal communication. *R/V Thomas G. Thompson*, Mauna Loa Plume Cruise, 2002.

P. Lonsdale. Tectonic and magmatic ridges in the Eltanin Fault System, south Pacific. *Mar. Geophys. Res.*, 8:203–242, 1986.

P. Lonsdale. Geography and history of the Louisville hotspot chain in the southwest Pacific. *J. Geophys. Res*, 93(B4):3078–3104, 1988.

P. Lonsdale and K. D. Klitgord. Structure and tectonic history of the eastern Panama basin. *Bull. geol. Soc. Am.*, 89:981–999, 1978.

A. Malahoff, R. H. Feden, and H. S. Fleming. Margnetic anomalies and tectonic fabric of marginal basins north of New Zealand. *J. Geophys. Res*, 87:4109–4125, 1982.

J. Mammerickx. The Foundation seamounts: tectonic setting of a newly discovered seamount chain in the south Pacific. *Earth Planet. Sci. Lett.*, 113:293–306, 1992.

D. P. Mattey. The minor and trace element geochemistry of volcanic rocks from Truk, Ponape and Kusaie, Eastern Caroline Islands: The evolution of a young hotspot trace across old Pacific Ocean crust. *Contrib. Mineral. Petrol.*, 80:1–13, 1982.

M. W. McElhinney. *Paleomagnetism and Plate Tectonics*. Cambridge, London, 1 edition, 1973.

P. Molnar and J. Stock. Relative motions of hotspots in the Pacific, Atlantic and Indian oceans since late Cretaceous time. *Nature*, 327:587–591, 1987.

J. G. Moore and D. A. Clague. Volcano growth and evolution of the island of Hawaii. *Geol. Soc. Am. Bull.*, 104:1471–1484, 1992.

J. G. Moore, D. A. Clague, and W. R. Normark. Diverse basalt types from Loihi seamount, Hawaii. *Geology*, 10:88–92, 1982.

W. J. Morgan. Convection plumes in the lower mantle. *Nature*, 230:43–44, 1971.

W. J. Morgan. Plate motions and deep mantle convection. *Geol. Soc. Am. Mem.*, 132:7–22, 1972.

R. D. Muller, J. Y. Royer, and L. A. Lawver. Revised plate motions relative to the hotspots from combined Atlantic and Indian Ocean hotspot tracks. *Geology*, 16:275–278, 1993.

C. R. Neal, J. J. Mahoney, L. W. Kroenke, R. A. Duncan, and M. G. Petterson. The Ontong Java plateau. In *Large Igneous Provinces: Continental, Oceanic, and Planetary Flood volcanism, Geophys. Monogr. Ser.*, volume 100, pages 183–216. AGU, Washington, D. C., 1997.

I. O. Norton. Plate motions in the north Pacific: The 43 ma nonevent. *Tectonics*, 14(5): 1080–1094, 1995.

I. O. Norton. Global hotspot reference frames and plate motion. In M. A. Richards, R. G. Gordon, and R. D. van der Hilst, editors, *The History and Dynamics of Global Plate Motions*, volume 121 of *Geophysical Monongraph Series*, pages 339–358. American Geophysical Union, 2000.

J. M. O'Connor, P. Stoffers, and J. R. Wijbrans. Migration rate of volcanism along the Foundation chain, SE Pacific. *Earth Planet. Sci. Lett.*, 164:41–59, 1998.

J. M. O'Connor, P. Stoffers, and J. R. Wijbrans. En-echelon volcanic elongate ridges connecting intraplate Foundation chain volcanism to the Pacific-Antarctic spreading center. *Earth Planet. Sci. Lett.*, 189:93–102, 2001.

E. A. Okal, D. F. Woods, and T. Lay. Intraplate deformation in the Samoa-Gilbert-Ralik area; a prelude to a change of plate boundaries in the southwest Pacific? *Tectonophysics*, 132:69–77, 1986.

K. Okino, S. Kasuga, and Y. Ohara. A new scenario of the Parece Vela basin genesis. *Mar. Geophys. Res.*, 20:21–40, 1998.

K. Okino, Y. Ohara, S. Kasuga, and Y. Kato. The Philippine Sea: New survey results reveal the structure and the history of the marginal basins. *Geophys. Res. Lett.*, 26(15): 2287–2290, 1999.

M. G. Petterson, C. R. Neal, J. J. Mahoney, L. W. Kroenke, A. D. Saunders, T. L. Babbs, R. A. Duncan, D. Tolia, and B. McGrail. Structure and deformation of north and central Malatia, Solomon Islands: tectonic implications for the Ontong Java Plateau-Solomon Arc collision, and for the fate of oceanic plateaus. *Tectonophysics*, 283:1–33, 1997.

F. Pollitz. Pliocene change in Pacific-plate motion. *Nature*, 320:738–741, 1986.

J. M. Rhodes. Personal communication. *R/V Thomas G. Thompson*, Mauna Loa Plume Cruise, 2002.

J. M. Rhodes, C. Morgan, and R. A. Liias. Geochemistry of axial seamount lavas: magmatic relationship between the Cobb hotspot and the Juan de Fuca ridge. *J. Geophys. Res.*, 95(B8):12,713–12,733, 1990.

N. M. Ribe and U. R. Christensen. The dynamical origin of Hawaiian volcanism. *Earth Planet. Sci. Lett.*, submitted, 1999.

D. H. Richter, J. G. Smith, M. A. Lanphere, G. B. Dalrymple, B. L. Reed, and N. Shew. Age and progression of volcanism, Wrangell volcanic field, Alaska. *Bull. Volcanology*, 53:29–44, 1990.

M. P. Ryan. The mechanics and 3-dimensional internal structure of active magmatic systems - Kilauea Volcano, Hawaii. *J. Geophys. Res. Sol*, 93(B5):4213–4220, 1988.

W. W. Sager and A. A. P. Koppers. Late Cretaceous Polar Wander of the Pacific Plate: Evidence of a Rapid True Polar Wander Event. *Science*, 287:455–459, 2000.

D. T. Sandwell and W. H. F. Smith. Marine gravity anomaly from Geosat and ERS-1 satellite altimetry. *J. Geophys. Res.*, 102(B5):10,039–10,054, 1997.

W. D. Sharp and D. A. Clague. A new older age of 47 Ma for the Hawaiian-Emperor Bend. *EOS, Trans. Am. Geophys. Union*, 80(46), 1999.

W. D. Sharp and D. A. Clague. An older, slower Hawaii-Emperor Bend. *EOS, Trans. Am. Geophys. Union*, 83(47), 2002.

W. H. F. Smith and D. T. Sandwell. Global sea floor topography from satellite altimetry and ship depth soundings. *Science*, 277(5334):1956–1962, 1997.

B. Steinberger. Plumes in a convecting mantle: models and observations for individual hotspots. *J. Geophys. Res.*, 05(B5):11,127–11,152, 2000.

B. Steinberger and R. J. O'Connell. Effects of mantle flow on hotspot motion. In M. A. Richards, R. G. Gordon, and R. D. van der Hilst, editors, *The History and Dynamics of Global Plate Motions*, volume 121 of *Geophysical Monongraph Series*, pages 377–398. American Geophysical Union, 2000.

J. A. Tarduno and R. D. Cottrell. Paleomagnetic evidence for motion of the Hawaiian hotspot during formation of the Emperor seamounts. *Earth Planet. Sci. Lett.*, 153:171–180, 1997.

J. A. Tarduno, R. A. Duncan, D. W. Scholl, R. D. Cottrell, B. Steinberger, T. Thordarson, B. C. Kerr, C. L. Neal, F. A. Frey, and C. Torii, M. Carvallo. The Emperor Seamounts: Southward Motion of the Hawaiian Hotspot Plume in Earth's Mantle. *Sciencexpress*, pages 1–6, 2003.

B. Taylor. Bismarck sea: Evolution of a back-arc basin. *Geology*, 7:171–174, 1979.

B. Taylor, A. Goodliffe, F. Martínez, and R. Hey. Continental rifting and initial sea-floor spreading in the Woodlark basin. *Nature*, 374:534–537, 1995.

S. F. Tebbens and S. C. Cande. southeast Pacific tectonic evolution from Early Oligocene to present. *J. Geophys. Res.*, 102(B6):12,061–12,084, 1997.

S. F. Tebbens, S. C. Cande, L. Kovacs, J. C. Parra, J. L. LaBrecque, and H. Vergara. The Chile Ridge: A tectonic framework. *J. Geophys. Res.*, 102(B6):12,035–12,059, 1997.

U. S. ten Brink and T. M. Brocher. Multichannel seismic evidence for a subcrustal intrusive complex under Oahu and a model for Hawaiian volcanism. *J. Geophys. Res.*, 92(B13): 13,687–13,707, 1987.

A. A. Tikku and S. C. Cande. The oldest magnetic anomalies in the Australian-Antarctic basin: Are they isochrons? *J. Geophys. Res.*, 104(B1):661–677, 1999.

M. Tivey. Personal communication. *R/V Thomas G. Thompson*, Jurassic Quiet Zone Cruise, 2002.

T. H. Torsvik, R. Van der Voo, and T. F. Redfield. Relative hotspot motions versus True Polar Wander. *Earth Planet. Sci. Lett.*, 202:185–200, 2002.

F. Trusdell. Personal communication. *R/V Thomas G. Thompson*, Mauna Loa Plume Cruise, 2002.

D. L. Turner, R. D. Jarrard, and R. B. Forbes. Geochronology and origin of the Pratt-Welker seamount chain, Gulf of Alaska: a new pole of rotation for the Pacific plate. *J. Geophys. Res.*, 85:6547–6556, 1980.

G. P. L. Walker. Geology and Volcanology of the Hawaiian Islands. *Pacific Science*, 44: 315–347, 1990.

P. Wessel and L. W. Kroenke. Relocating Pacific hot spots and refining absolute plate motions using a new geometric technique. *Nature*, 387(6631):365–369, 1997.

P. Wessel and L. W. Kroenke. The geometric relationship between hot spots and seamounts: Implications for Pacific hot spots. *Earth Planet. Sci. Lett.*, 158:1–18, 1998.

P. Wessel and S. Lyons. Distribution of large Pacific seamounts from Geosat/ERS-1: implications for the history of intraplate volcanism. *J. Geophys. Res.*, 102(B10):22,459–22,476, 1997.

P. Williamson. Recent studies of Macquarie Island and the Macquarie Ridge Complex. *Bull. Austr. Soc. Expl. Geophys.*, 5:19–22, 1974.

J. T. Wilson. A possible origin of the Hawaiian islands. *Can. J. Phys.*, 41:863–870, 1963.

J. T. Wilson. A new class of faults and their bearing on continental drift. *Nature*, 207: 343–347, 1965.

M. L. Zoback, M. H. McKee, and R. J. Blakely. The northern Nevada rift: Regional tectono-magmatic relations and middle Eocene stress direction. *Geol. Soc. Am. Mem.*, 106(3):371–382, 1994.